

Discovery of a parenteral small molecule coagulation Factor XIa inhibitor clinical candidate (BMS-962212)

Donald J. P. Pinto, Michael J. Orwat, Leon M. Smith II, Mimi L Quan, Patrick Y. S. Lam, Karen A Rossi, Atsu Apedo, Jeffery M. Bozarth, Yiming Wu, Joanna J Zheng, Baomin Xin, Nathalie Toussaint, Paul Stetsko, Olafur Gudmundsson, Brad D. Maxwell, Earl J Crain, Pancras C Wong, Zhen Lou, Timothy W. Harper, Silvi A Chacko, Joseph E Myers, Steven Sheriff, Huiping Zhang, Xiaoping Hou, Arvind Mathur, Dietmar A Seiffert, Ruth R. Wexler, Joseph M Luetttgen, and William R Ewing
J. Med. Chem., **Just Accepted Manuscript** • DOI: 10.1021/acs.jmedchem.7b01171 • Publication Date (Web): 27 Oct 2017

Downloaded from <http://pubs.acs.org> on October 29, 2017

Just Accepted

“Just Accepted” manuscripts have been peer-reviewed and accepted for publication. They are posted online prior to technical editing, formatting for publication and author proofing. The American Chemical Society provides “Just Accepted” as a free service to the research community to expedite the dissemination of scientific material as soon as possible after acceptance. “Just Accepted” manuscripts appear in full in PDF format accompanied by an HTML abstract. “Just Accepted” manuscripts have been fully peer reviewed, but should not be considered the official version of record. They are accessible to all readers and citable by the Digital Object Identifier (DOI®). “Just Accepted” is an optional service offered to authors. Therefore, the “Just Accepted” Web site may not include all articles that will be published in the journal. After a manuscript is technically edited and formatted, it will be removed from the “Just Accepted” Web site and published as an ASAP article. Note that technical editing may introduce minor changes to the manuscript text and/or graphics which could affect content, and all legal disclaimers and ethical guidelines that apply to the journal pertain. ACS cannot be held responsible for errors or consequences arising from the use of information contained in these “Just Accepted” manuscripts.



1
2
3
4
5
6
7
8
9
10
11
12
13
14
15
16
17
18
19
20
21
22
23
24
25
26
27
28
29
30
31
32
33
34
35
36
37
38
39
40
41
42
43
44
45
46
47
48
49
50
51
52
53
54
55
56
57
58
59
60



Discovery of a parenteral small molecule coagulation Factor XIa inhibitor clinical candidate (BMS-962212)

Donald J. P. Pinto,* Michael J. Orwat, Leon M. Smith II, Mimi L. Quan, Patrick Y. S. Lam, Karen A. Rossi, Atsu Apedo, Jeffrey M. Bozarth, Yiming Wu, Joanna J. Zheng, Baomin Xin, Nathalie Toussaint, Paul Stetsko, Olafur Gudmundsson, Brad Maxwell, Earl J. Crain, Pancras C. Wong, Zhen Lou, Timothy W. Harper, Silvi A. Chacko, Joseph E. Myers Jr., Steven Sheriff, Huiping Zhang, Xiaoping Hou, Arvind Mathur, Dietmar A. Seiffert, Ruth R. Wexler, Joseph M. Luetzgen, William R. Ewing

Bristol-Myers Squibb Company, Research and Development, P.O. Box 5400, Princeton, New Jersey 08543, United States

ABSTRACT

Factor XIa (FXIa) is a blood coagulation enzyme that is involved in the amplification of thrombin generation. Mounting evidence suggests that direct inhibition of FXIa can block pathologic thrombus formation while preserving normal hemostasis. Preclinical studies using a variety of approaches to reduce FXIa activity, including direct inhibitors of FXIa, have demonstrated good antithrombotic efficacy without increasing bleeding. Based on this potential, we targeted our efforts at identifying potent inhibitors of FXIa with a focus on discovering an acute antithrombotic agent for use in a hospital setting. Herein we describe the discovery of a potent FXIa clinical candidate, **55** (FXIa $K_i = 0.7$ nM), with excellent preclinical efficacy in thrombosis models and aqueous solubility suitable for intravenous administration. **BMS-962212** is a reversible, direct, and highly selective small molecule inhibitor of FXIa.

INTRODUCTION

Cardiovascular (CV) disease continues to be the leading cause of death worldwide.^{1a} Thrombus formation in the arterial circulation can cause myocardial infarction or ischemic stroke. In the venous circulation, blood clots can cause local pain and swelling. A venous blood clot can break free and travel to the lungs causing a pulmonary embolism (PE) leading to sudden death. Together, myocardial infarction, ischemic stroke, and venous thromboembolism (VTE) account for a large portion of deaths due to cardiovascular disease.^{1a,b}

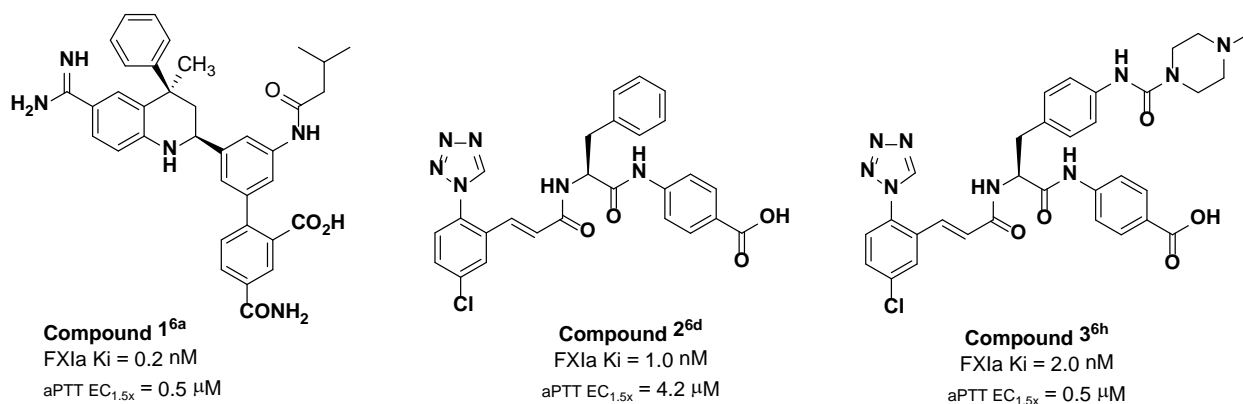
Oral anticoagulant and antiplatelet medicines are highly effective for the long-term prevention of thrombotic events.^{2a-d} However, in the acute phase, it is desirable to have an antithrombotic agent which can treat the event and prevent an early recurrence when the risk is known to be the highest. During this acute period, oral medicines are less suited because they require hours to achieve their maximum plasma concentration and therefore their maximum antithrombotic effect. Further, a long-acting oral antithrombotic is not preferred if the potential for an urgent surgical intervention is foreseeable or if the risk of hemorrhage outweighs the benefits. For decades, heparin has been the most widely used acute antithrombotic agent.³ Heparin accelerates the antithrombin III mediated inhibition of multiple blood coagulation proteases. Although heparin has a rapid onset of action and, relative to oral agents, a rapid offset of action, it has some properties which limit its use and effectiveness. Heparin requires dose titration which is often accomplished using the activated partial thromboplastin time (aPTT) targeted to achieve 1.5- to 2.5-times the normal aPTT. Overdose of heparin can cause serious bleeding complications. Repeated heparin administration in rare cases can cause heparin-induced thrombocytopenia (platelet consumption) which increases the risk of bleeding and other complications.

Factor XIa (FXIa) inhibition has emerged as a means to achieve anticoagulation without significant effects on hemostasis.^{4a} Human FXI deficiency (hemophilia C) was first described as a mild to moderate bleeding disorder.^{4b} However, these subjects rarely suffer from spontaneous bleeding episodes, and when bleeding does occur it most often is associated with trauma or surgery, especially in tissues with high fibrinolytic activity. Further, epidemiologic studies show an increased risk of thrombosis in subjects with elevated FXI levels and some protection from thrombosis in subjects with reduced FXI levels.^{4c,d} Preclinically, inhibition of FXIa as an effective antithrombotic approach came from studies in rats^{5a} and rabbits^{5b} with a FXIa active site directed irreversible inhibitor, and from studies in genetically modified FXI-deficient mice.^{5c,d} At Bristol-Myers Squibb we have developed a strategy to identify small molecule parenteral FXIa inhibitors that have the potential to address the high unmet medical need in the acute care setting. This strategy was strengthened with additional preclinical studies with other direct FXIa inhibitors,^{6a-n} antibodies which blocked FXI activation or FXIa activity,^{7a-c} and antisense oligonucleotides (ASO)^{8a,b} which blocked FXI synthesis. Furthermore our hypothesis to target FXIa inhibition was supported by a phase II clinical study with a FXI-directed ASO in subjects undergoing elective knee arthroplasty which showed that reducing FXI levels was an effective means to reduce thrombosis and also appeared to be safe with respect to bleeding.^{8c} Based on our preclinical data with small molecule FXIa inhibitors, and the recent clinical data with the ASO, the potential for FXIa inhibition to produce a superior antithrombotic profile with a low additional bleeding risk is a very appealing strategy to address the unmet medical need in the acute care setting.

We previously reported on a FXIa tool molecule **1** (FXIa Ki = 0.2 nM)^{6a} which was found to be highly efficacious in a rabbit electrically-mediated carotid arterial thrombosis (ECAT) model, with minimal increase in bleeding time at a dose that provided 80% inhibition of thrombosis.⁹ Recently,

we also reported on the discovery of a series of phenylalanine diamide FXIa inhibitors (e.g. compound **2**) having a *p*-chlorophenyltetrazole P1 group and a *p*-aminobenzoic acid P2' moiety.^{6d} Extensive SAR within this series culminated in the identification of an extended piperazine P1' urea analog, **3** (FXIa K_i = 2 nM), with excellent anticoagulant activity (aPTT $IC_{1.5x}$ = 0.50 μ M) and antithrombotic efficacy (EC_{50} = 2.8 μ M) in a rabbit ECAT thrombosis model.^{6h} Compound **3** was a highly polar zwitterionic molecule with poor aqueous solubility and not suitable for further evaluation. Herein, we describe our continuing efforts directed at identifying a first small molecule parenteral FXIa inhibitor which culminated in a Phase I clinical candidate.

Figure-1: Novel FXIa inhibitors identified at Bristol-Myers Squibb

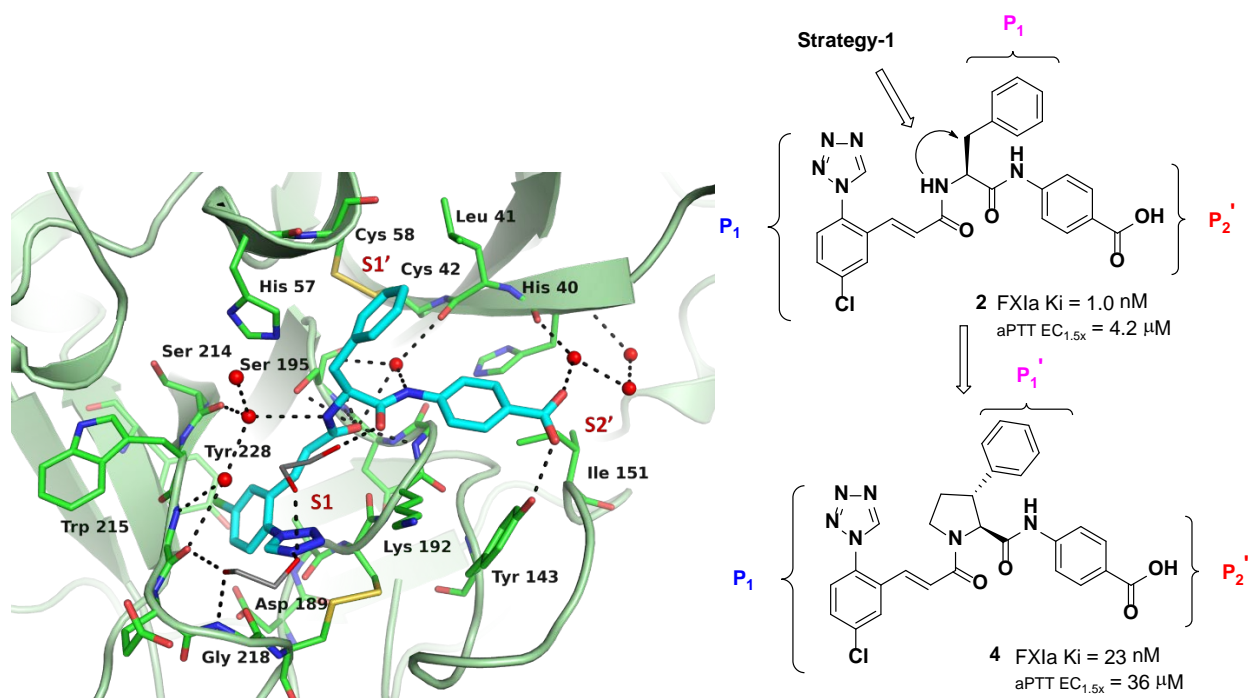


RESULTS AND DISCUSSION

Our initial attempts at improving solubility and in vitro anticoagulant activity within the phenylalanine chemotype proved to be challenging. However, based on the FXIa bound x-ray structure for compound **2**,^{6d} we reasoned that the potential existed for discovering an alternative scaffold, which would allow us to incorporate functionalities to provide adequate solubility without compromising on the FXIa potency. We began this effort by closely examining the FXIa bound x-ray structure for compound **2**. Some of the key attributes for inhibitor **2** are (1) the

chlorophenyltetrazole acrylamide P1 that enables the chlorine and the tetrazole moieties to occupy the S1 pocket making key interactions with Tyr 228 at the bottom of the pocket and the disulfide at the top of the S1 pocket, (2) the acrylamide linker that places the amide carbonyl such that it directly interacts with enzyme residues in the oxyanion region, while the carboxamide NH (which is attached to the P2' benzoic acid group) interacts with a conserved water, (3) the benzoic acid P2' group that forms a strong interaction with Tyr 143 and His 40 and (4) the phenyl moiety of the phenylalanine that is within contact distance of the disulfide bridge in the S1' region.

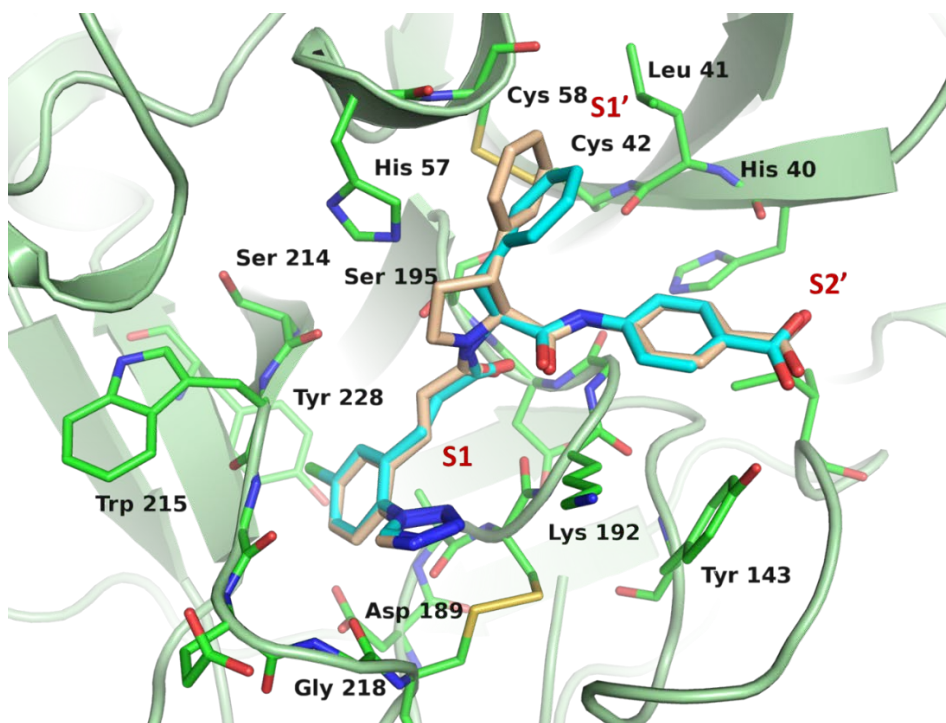
Figure-2: FXIa bound x-ray structure of phenylalanine analog **2** (3.3 Å, PDB 5E2O)^{6h}



The benzylic carbon bearing the P1' phenyl group and the acrylamide NH appeared to be in the same plane. This observation prompted us to determine whether we could connect these two atoms in the form of a proline. A careful look at the proline scaffold model for compound **4** showed that relative to compound **2**, this connectivity would be a viable approach without significantly altering the overall conformation and binding to FXIa. Indeed, compound **4**,

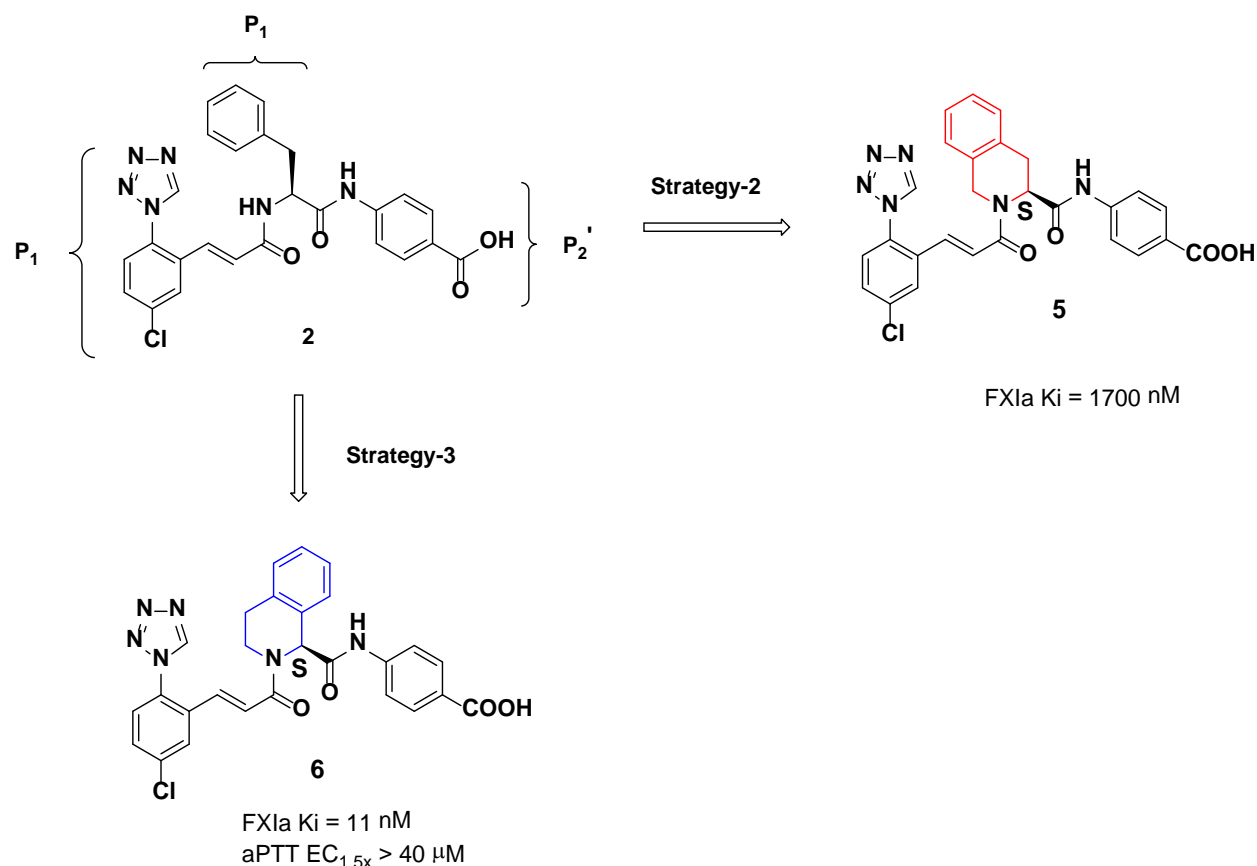
showed modest FXIa binding affinity (FXIa K_i = 23 nM). Figure-3 shows an overlay of the FXIa bound x-ray structures for compound **2** and proline analog **4**. While the orientation of the P1 groups are similar in the S1 pocket for **2** and **4**, some subtle binding changes were seen elsewhere which may account for the decrease in binding affinity. For example, the acrylamide linker carbonyl oxygen atom interaction with oxyanion hole residue Gly 193 differs slightly between **2** and **4** (~3.0 Å for compound **4** and ~2.7 Å for compound **2**). The incorporation of the proline scaffold in **4** positions the 3(*R*)-phenyl P1' group to be in close proximity to His 57, eliciting an edge to face interaction and also appears to be slightly extended over the disulfide bridge. In contrast, for compound **2**, a slight twist of the phenylalanine P1' group is observed relative to compound **4**. In the S2' region, the benzoic acid P2' group in **4** appears to be slightly extended relative to compound **2**. Various substitutions were made on the proline linked P1' phenyl ring, but none afforded potencies that were better than compound **4**.

Figure-3: Overlay of x-ray structures of compound **2** (3.3 Å; PDB 5E2O) (**blue**) and **4** (2.9 Å; PDB 5QCK) (**brown**) in the active site of FXIa.



To address the potency issue, we embarked on another strategy (Figure-4). This strategy relied on a connectivity that involved the phenyl P1' group and the acrylamide nitrogen as shown in Figure-4. This concept generated isomeric tetrahydroisoquinoline (THIQ) scaffolds (Figure-4; strategy 2 and 3, compounds **5** and **6**). The computational and modeling experiments suggested that the THIQ scaffold **6** would be best suited for this purpose and could make several key FXIa

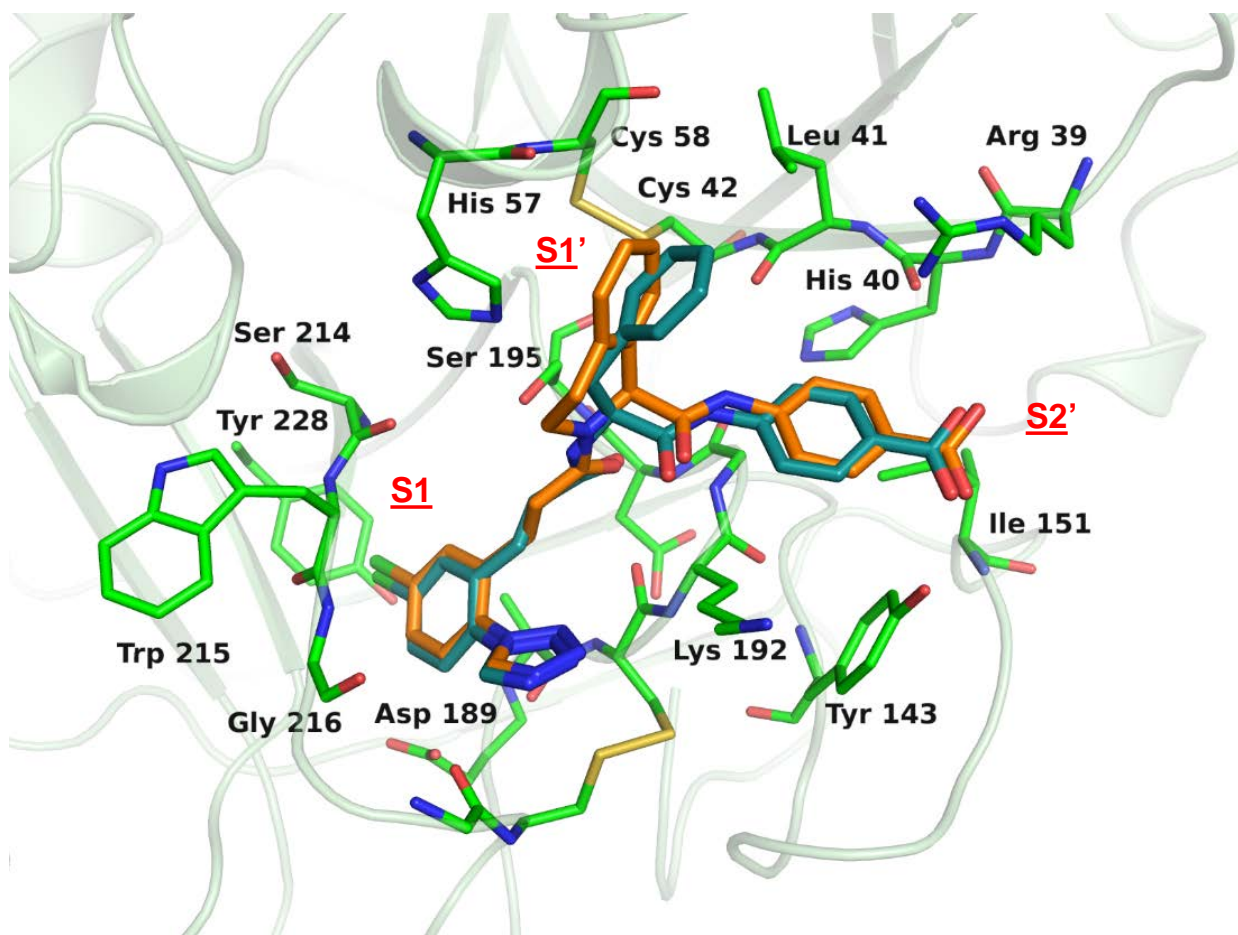
Figure-4: Evolution of the tetrahydroisoquinoline (THIQ) FXIa scaffold.



interactions previously seen with **2** and **4**. To test this hypothesis, homochiral compounds **5** and **6** were prepared. We were delighted that compound **6** (FXIa K_i = 11 nM) performed as predicted by our computational study and was significantly more potent than **5** (FXIa K_i = 1700 nM). Figure-5 shows an overlay of the FXIa bound x-ray structure of **6** (2.11 Å) with **2**, from which it can be seen that the location of the chiral center in **6** is shifted relative to compound **2**. One plausible explanation for this observation was that, in order to accommodate the rigid THIQ scaffold, a slight shift in the orientation of **6** in the FXIa active site was necessary. This change also resulted in the benzoic acid P_2' group in **6** being extended slightly into the S_2' region. Importantly, the change notwithstanding, the highly constrained THIQ scaffold maintained all the binding interactions seen previously with compounds **2** and **4** in the FXIa binding site, and additionally the scaffold formed an edge to face interaction with His 57 and also appears to engage the Cys 42 - Cys 58 disulfide

residues in the S1' region. Although the potency changes were not significant at this juncture, the overall strategy of incorporating a novel THIQ scaffold proved invaluable for further optimization.

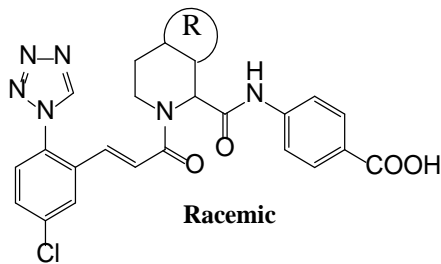
Figure-5: Overlay of FXIa bound x-ray structures **2** (3.3 Å; PDB 5E2O) (**blue**) and **6** (2.11 Å; PDB 5QCL) (**brown**)



The encouraging FXIa data obtained for **6** prompted us to also evaluate a select set of 5 and 6-membered heterobicyclic THIQ analogs (Table-1). The 5,6,7,8-tetrahydro-1,6-naphthyridine **7** (FXIa K_i = 56 nM) and 1,2,3,4-tetrahydro-2,7-naphthyridine **8** (FXIa K_i = 160 nM) were weaker relative to **6**, but were within 3-fold of each other in terms of potency. From the 5,6-heterobicyclic chemotype, the unsubstituted 4,5,6,7-tetrahydro-2H-pyrazolo[4,3-c]pyridine **9** (FXIa K_i = 640 nM) was significantly less potent. Although the NH of **9** provided us with an opportunity for

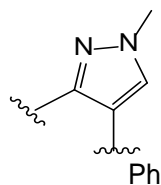
substitution at this position, we hypothesized that the shallow S1' pocket would not allow for bulky substitutions. To test this hypothesis, we prepared the 2-methyl analog **10**, which shows a modest 3-fold improvement in FXIa binding affinity relative to **9**; whereas the 2-phenyl (**11**) and 2-benzyl (**12**) analogs were much weaker in line with our modeling predictions. The 2,3-dimethyl analog **13** (FXIa K_i = 29 nM) showed comparable binding affinity to **6**, although a loss in affinity was seen for the regioisomeric analogs **14** (FXIa K_i = 80 nM) and **15** (FXIa K_i = 300 nM). This limited SAR for alternative THIQ scaffolds appeared to favor compound **6** for further optimization studies.

Table-1: 5, and 6-Membered heterobicyclic THIQ replacements



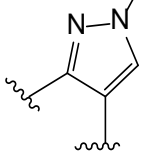
| Compound | R | ^a FXIa K_i nM |
|----------------------|---|----------------------------|
| 6 (chiral) | | 11 |
| 7 | | 51 |
| 8 | | 160 |
| 9 | | 640 |

10



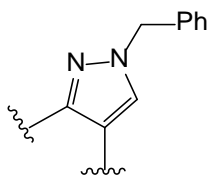
270

11



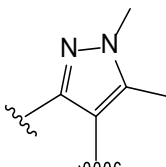
2000

12



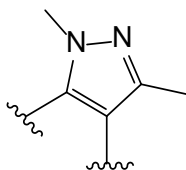
1400

13



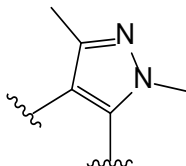
29

14



80

15



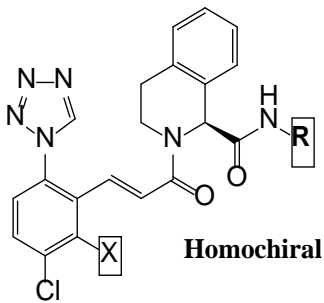
300

^aK_i values were obtained from purified human enzyme at 25 °C and were averaged from multiple determinations (n=2), as described in Ref. 6c.

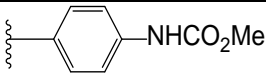
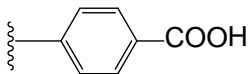
We next focused on exploring alternative P2' groups (Table-2). It was interesting to note that the *meta*-benzoic acid compound **16** was ~26-fold less active when compared to **6**. We also explored the methylcarbamate and indazole P2' groups previously identified in the phenylimidazole series of compounds.^{6c} The carbamate P2' containing compounds **17** and **18** showed a significant loss in FXIa potency. A similar finding was also found for indazole compounds **19** and **20**, suggesting the

location of the carbamate and indazole P2' moieties in the S2' pocket are slightly altered resulting in weaker interactions with the enzyme residues in this region.

Table-2: P2' THIQ structure activity relationships



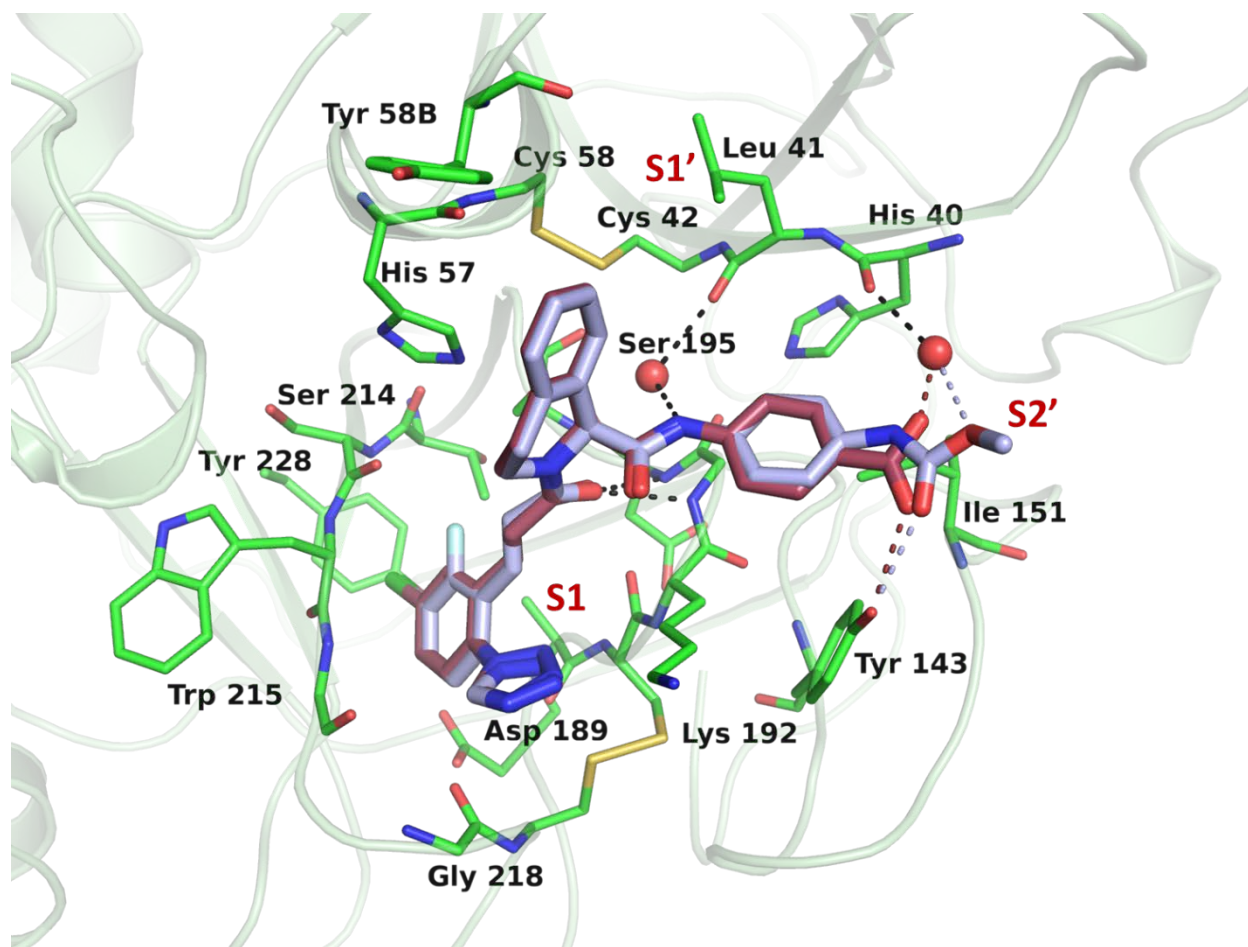
| Compound | X | R | ^a FXIa Ki nM |
|----------|---|---|-------------------------|
| 6 | H | | 11 |
| 16 | H | | 290 |
| 17 | H | | 870 |
| 18 | H | | 890 |
| 19 | H | | 57 |
| 20 | H | | 83 |

| | | | |
|-----------|----------|---|------------|
| 21 | F |  | 110 |
| 22 | F |  | 3.7 |

^aK_i values were obtained from purified human enzyme at 25 °C and were averaged from multiple determinations (n=2), as described in Ref. 6c.

The proline compound **4** and the THIQ **6** show that the 4-chlorophenyltetrazole P1 group, which was carefully optimized for the diamide **2**, is effective in other chemotypes such as in the phenylalanine series.^{6d,6h} Additionally in the phenylalanine series, we had observed that subtle changes on the P1 phenyl group such as incorporation of a fluoro group adjacent to the 4-Cl moiety impacted the FXIa potency.^{6h} The introduction of a 3-fluoro-4-chlorophenyltetrazole P1 in **21** (FXIa K_i = 110 nM, Table-2) afforded an 8-fold improvement in FXIa binding compared to **17** lacking the 3-fluoro substituent. A similar trend was also observed for **22** (FXIa K_i = 3.7 nM) relative to **6**. To understand this improvement in potency, we obtained the FXIa bound structure for compound **21** and compared it with the bound conformation of **6** (Figure-6). Not too surprisingly, the P1 4-chloro group in **21** engages the Tyr 228 residue, while the adjacent 3-fluoro moiety appears to be in close contact with Thr 213 (3.0 Å). This interaction could in part result in the slight potency gain seen with the 3-fluoro-4-chlorophenyltetrazole P1 in **21**. For the S2' interactions, the carbamate P2' group in **21** appears to orient above the benzoic acid group in **6**. The slight shift in the orientation of the carbamate group potentially weakens the interactions with the enzyme residues in the S2' region, even though a close contact of the carbamate carbonyl and Tyr 143 (2.8 Å), and a corresponding network water interaction with His 40 is observed.

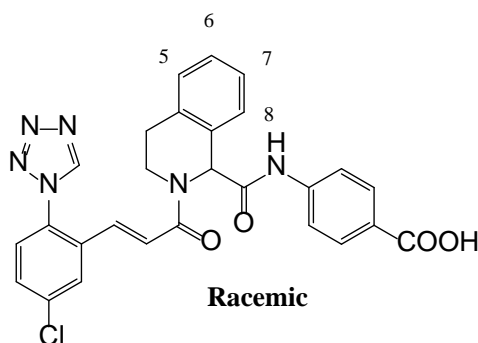
Figure-6: An overlay of the FXIa bound x-ray structures of compound **6** (2.1 Å; PDB 5QCL) (**red**) and **21** (2.2 Å; PDB 5QCM) (**purple**).



The orientation of the THIQ scaffold in the FXIa enzyme S1' pocket provided us with a unique opportunity to explore substitutions on this scaffold. Figure-6 shows the THIQ in **21** to be in close proximity to the disulfide in the S1' region, such that substitution at either the 7 or 8 positions of the THIQ ring would result in a steric clash. On the other hand, substitutions at either the 5 or 6 positions of the THIQ seemed feasible, though some steric clash with the S1' residues with substitution at the 6 position of the THIQ could not be ruled out. Substitution at the 5-position of the THIQ appeared to project into the S2 pocket of the FXIa active site. To test this hypothesis, we prepared the select set of compounds listed in Table-3. From this initial set, the compounds that showed promise were indeed the 5-substituted compounds, such as the dimethylamino

compound **25** (FXIa K_i = 6 nM), methoxycarbonyl compound **23** (FXIa K_i = 17 nM) and cyano compound **24** (FXIa K_i = 39 nM). The FXIa affinity of the dimethylamino compound **25** was the most encouraging. Based on the availability of the THIQ scaffolds, we explored a relatively small set of compounds with substitutions at positions 6, 7 and 8 on the THIQ ring. From this set it was clear that a small substituent at the 6-position of the THIQ, such as the 6-methyl **27** was comparable to compound **6** in terms of potency, but larger groups as in the 6-methylester analog **26** resulted in a loss of FXIa affinity.

Table-3: Exploratory THIQ scaffold substitutions



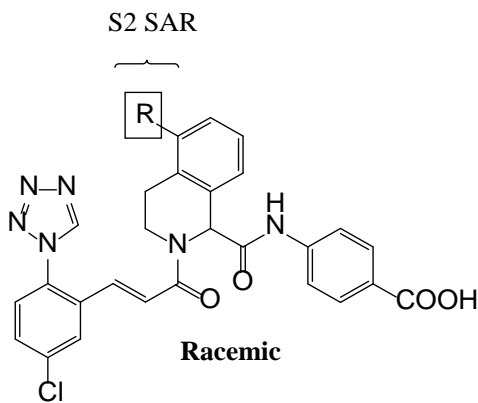
| Compound | R | FXIa ^a K _i nM |
|-------------------|---------------------------|-------------------------------------|
| 6 (chiral) | H | 11 |
| 23 | 5-CO₂Me | 17 |
| 24 | 5-CN | 39 |
| 25 | 5-NMe₂ | 6 |
| 26 | 6-CO₂Me | 140 |
| 27 | 6-Me | 27 |
| 28 | 7-CO₂Me | 230 |
| 29 | 7-CN | 400 |
| 30 | 7-Me | 28 |
| 31 | 8-CO₂Me | 2200 |

^aK_i values were obtained from purified human enzyme at 25 °C and were averaged from multiple determinations (n=2), as described in Ref. 6c.

Other substitutions at either the 7 or 8 positions of the THIQ ring also showed a loss in FXIa affinity relative to compound **6**. We were delighted with these results as it validated our hypothesis

for substitution on the THIQ scaffold. Importantly, compound **25** opened up the possibility for an extensive SAR at the previously unexplored S2 pocket of FXIa via substitution at the 5-position of the THIQ to probe for additional binding interactions.

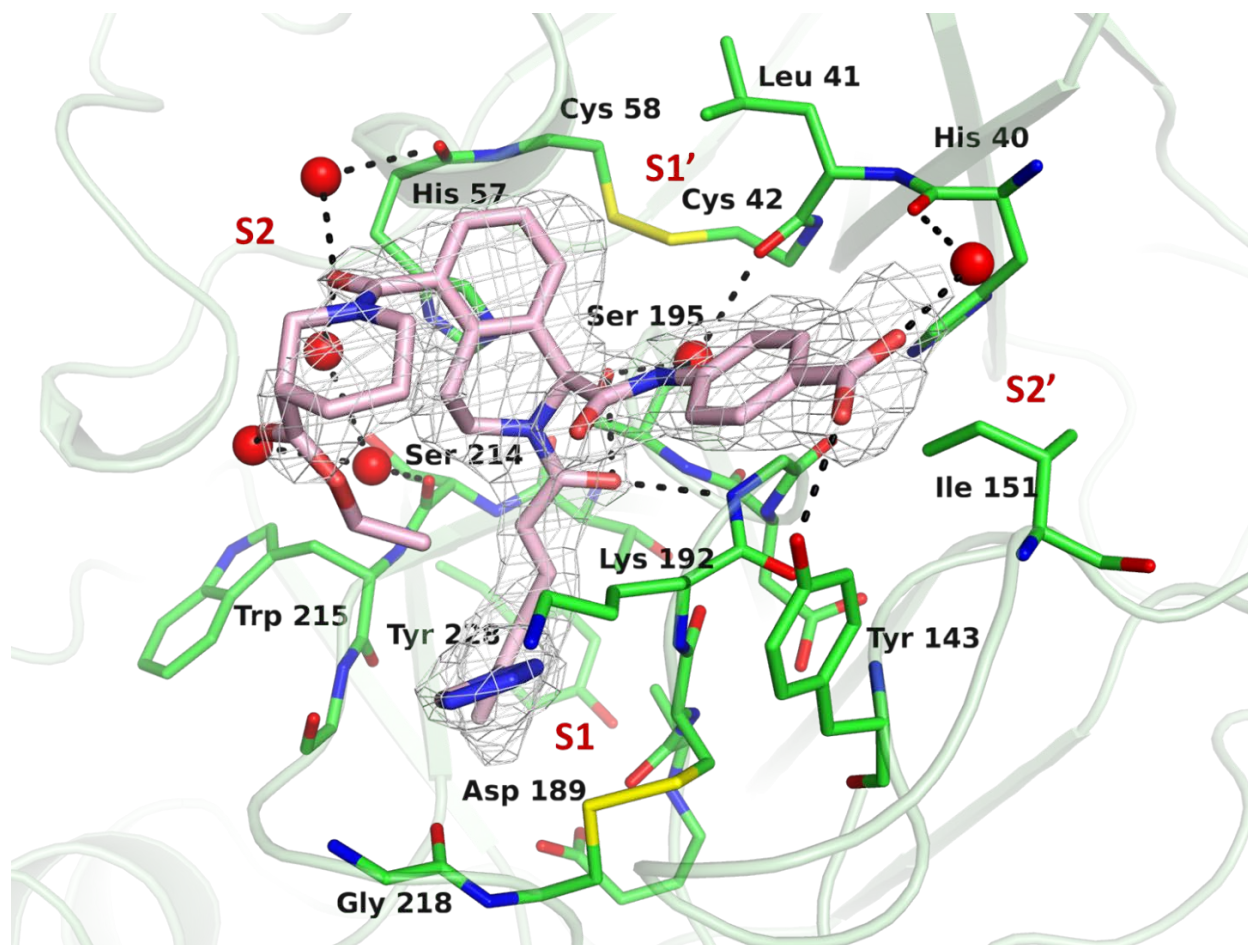
Table-4: Effect of electron withdrawing groups at the 5-position of THIQ scaffold – S2 SAR



| Compound | R | ^a FXIa Ki nM |
|-----------|--------------------|-------------------------|
| 23 | CO ₂ Me | 17 |
| 32 | COOH | 74 |
| 33 | CONMe ₂ | 25 |
| 34 | | 27 |
| 35 | | 17 |
| 36 | | 18 |
| 37 | | 12 |
| 38 | | 6 |

^aK_i values were obtained from purified human enzyme at 25 °C and were averaged from multiple determinations (n=2), as described in Ref. 6c.

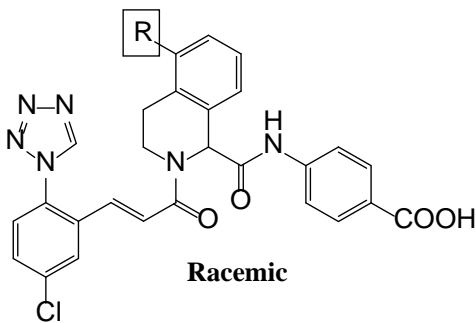
Figure-7: FXIa bound x-ray structure of compound **38** (2.3 Å; PDB 5QCN)



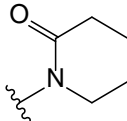
At first we explored the effectiveness of a select set of carboxamido groups (compounds **33-38**) at the 5-position of the scaffold (Table-4). In general, the FXIa affinities were comparable to that observed for compound **23**; however, the carboxamide **38** (FXIa $K_i = 6$ nM) was approximately 2-3 fold better. The 5-carboxylic acid **32** had ~4-fold less FXIa affinity when compared to the corresponding ester compound **23**. An FXIa bound x-ray structure for compound **38** (2.30 Å) was obtained (Figure-7). The S2 region of the FXIa enzyme shows an array of water molecules. The P2 carboxamide compound **38** appears to derive its potency by engaging these water molecules. The carbonyl oxygen of the piperidinyl carboxylate interacts with the S2 enzyme residues through a network of waters. While this is an intriguing find, it is also interesting to

note that **38** and the dimethylamino analog **25** (FXIa K_i = 6 nM, Table-3) display similar FXIa affinities.

Table-5: A selection of 5-amino substituted THIQ analogs.



| Compound | R | ^a FXIa K_i nM | aPTT IC 1.5x μ M |
|-----------|----------------------|----------------------------|----------------------|
| 25 | | 6 | >40 |
| 39 | | 21 | 26 |
| 40 | NHCO ₂ Me | 23 | >40 |
| 41 | | 25 | 22 |
| 42 | | 17 | >40 |
| 43 | | <5 | 0.65 |
| 44 | | <5 | 11 |

| | | | |
|----|---|-----|----|
| 45 |  | 5.8 | 39 |
|----|---|-----|----|

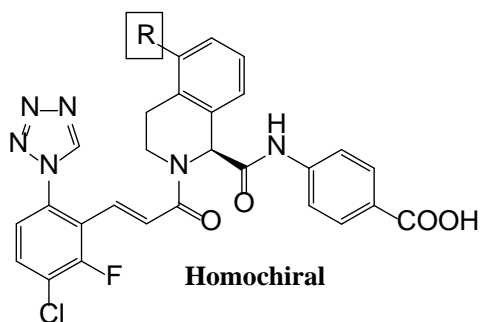
^aK_i values were obtained from purified human enzyme at 25 °C and were averaged from multiple determinations (n=2), as described in Ref. 6c. aPTT (activated partial thromboplastin time) in vitro clotting assay was performed in human plasma as described in reference 6c.

Encouraged by similar results for compounds containing either a carboxy or an amino P2 substituent as reflected by the FXIa potencies for compounds **25** and **38**, we explored additional 5-substituted amino P2 containing compounds (Table-5). The less basic compounds such as the acetamide and urea P2 compounds **39-42** showed a 3-4-fold loss in FXIa binding affinity relative to the dimethylamino compound **25**, while the more polar 5-piperazine containing compound **43** (FXIa K_i < 5 nM) was significantly better. Compound **43** also showed excellent anticoagulant activity in the clotting assay (aPTT IC_{1.5x} = 0.65 μM). A similar finding was also observed with the piperazine carbamate compound **44**, although its clotting activity was much weaker. The effect of basicity on FXIa affinity and clotting activity is further accentuated by the observation that the lactam P2 analog **45** (FXIa K_i 5.8 nM, aPTT IC_{1.5x} = 39 μM) displayed good FXIa affinity, but also showed weak anticoagulant activity. Compound **43** at this juncture, exhibited the characteristics suitable for a parenteral agent in terms of potency but to advance into further studies acceptable solubility was required. The solubility was measured (< 5 μg/ml) and determined to be low for its amorphous form. The poor solubility trends were a characteristic feature for a number of compounds in Table-5. The racemic THIQ P2 compounds as in Table-5 allowed us to rapidly identify key functional groups and trends that could be further exploited with homochiral compounds.

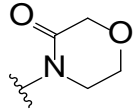
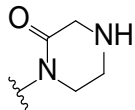
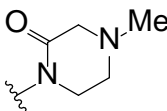
The THIQ analogs that were substituted at the 5-position allowed us to reach our FXIa potency and the in vitro anticoagulant criteria. Moreover, we used the information shown in Table-5 to further our understanding of the SAR with the goal of achieving a highly potent compound with

good aqueous solubility. To do this, we incorporated the highly optimized 3-fluoro-4-chlorophenyltetrazole P1 group with homochiral THIQ scaffolds (Table-6). This resulted in the identification of highly potent FXIa compounds. Importantly, the THIQ scaffold allowed for the incorporation of a diverse set of P2 groups that were well tolerated in the active site of FXIa. For example, compounds that contained morpholine (**46**), thiomorpholine (**47**), sulfonyl (**48**) and piperidine (**49**) P2 groups had sub-nanomolar FXIa affinity, with the morpholine analog (**46**) also demonstrating good anticoagulant activity ($\text{aPTT}_{1.5x} = 0.9 \mu\text{M}$). A similar finding was also observed with the zwitterionic compounds, such as 4-dimethylamino piperidine compound **50** (FXIa $K_i = 0.1 \text{ nM}$, $\text{aPTT}_{1.5x} = 0.1 \mu\text{M}$), piperazinone analogs **54** and **55** and compounds such as spirolactam compound **51**, lactam **52**, and morpholinone **53**. The lactam containing compounds **52**, **53** and **55** all showed acceptable solubility at pH 6.4. Among these, compound **55** had the most balanced profile in terms of FXIa affinity, anticoagulant activity and amorphous aqueous solubility (pH 6.4 Sol = 0.88 mg/mL). Compound **55** represented a milestone compound for the parenteral program and had all the physical chemical properties we sought for advancing the compound into development.

A model of compound **55** (Figure-8) in the FXIa active site shows the P2 N-methylpiperazinone group making a lipophilic interaction with Tyr 94 and Tyr 58B. Additionally, the benzoic acid P2' and the chlorophenyltetrazole P1 groups make the requisite interactions at the S1 and S2' regions as previously described for similar compounds.

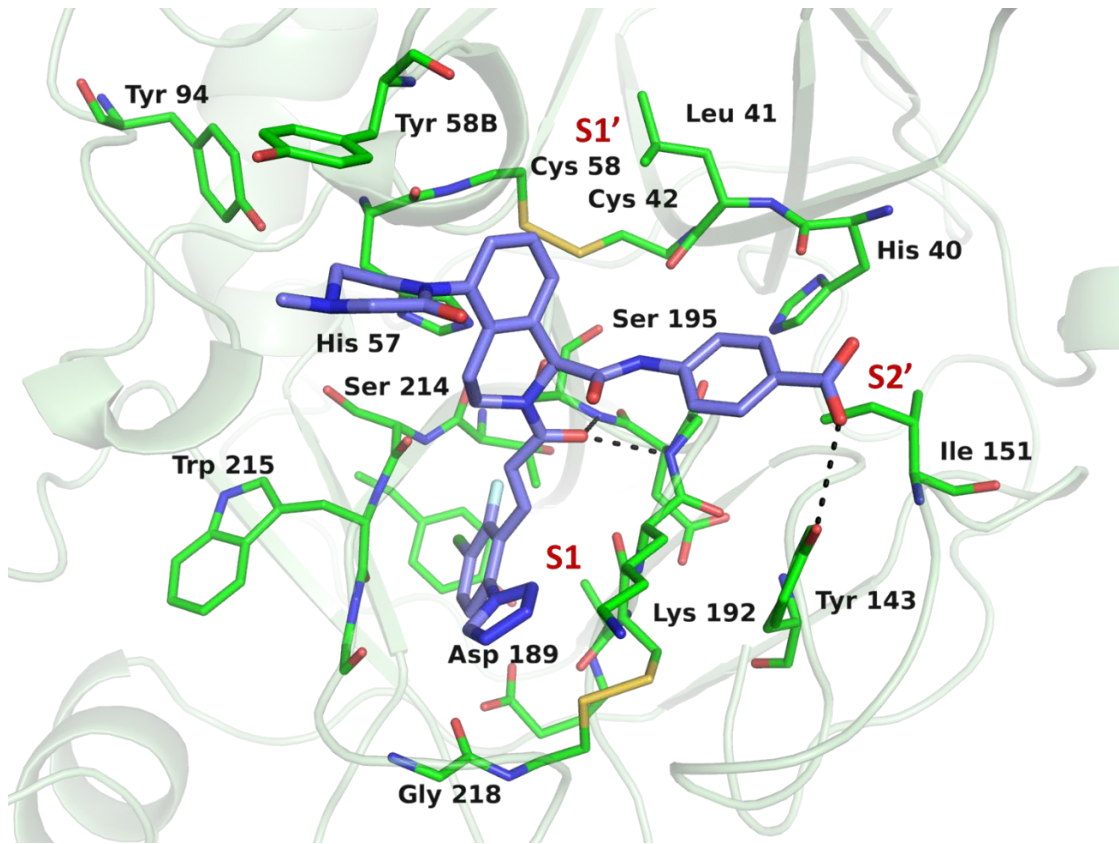
Table-6: The SAR 5-substituted heterocyclic P2 homochiral THIQ analogs.

| Compound | R | ^a FXIa K _i nM | aPTT IC ₅₀ 1.5x μM | Solubility @pH 6.5 mg/ml |
|----------|---|--|-------------------------------------|--------------------------------|
| 46 | | 0.38 | 0.91 | - |
| 47 | | 0.49 | 2.5 | - |
| 48 | | 2.0 | 29 | - |
| 49 | | 2.2 | 24 | - |
| 50 | | 0.098 | 0.11 | NT |
| 51 | | 0.07 | 0.45 | 0.094 |
| 52 | | 1.4 | 0.84 | 0.92 |

| | | | | |
|----|---|------|------|-------|
| 53 |  | 2.0 | 0.55 | 0.37 |
| 54 |  | 1.4 | 0.3 | 0.027 |
| 55 |  | 0.71 | 0.3 | 0.88 |

^aK_i values were obtained from purified human enzyme at 25 °C and were averaged from multiple determinations (n=2), as described in Ref. 6c. aPTT (activated partial thromboplastin time) in vitro clotting assay was performed in human plasma as described in reference 6c. NT = Not tested. All solubilities are from amorphous compounds.

Figure-8: A docked model of compound **55** in FXIa



PHARMACOKINETIC PROFILE FOR THIQ FXIa INHIBITORS

The compounds that were chosen for evaluation in rat PK studies (cassette dosing format, Table-7) satisfied the criteria we had established, i.e., potent FXIa binding, good anticoagulant activity as measured in the aPTT assay and adequate aqueous solubility. From this study we were seeking

compounds with short half-life (< 1 h) to instill a rapid onset and offset of pharmacology. Compound **50** showed low clearance values and also had a short half-life. Compounds **51-53** and **55**, had moderate clearance values and likewise demonstrated short half-lives in the desirable range. Compound **55** best met the pre-determined criteria of low to moderate clearance and a pharmacokinetic half-life of less than 1 h, and thus emerged as a potential leading candidate. The pharmacokinetic profile of **55** was subsequently evaluated in rats, dogs and cynomolgus monkeys (Table-8). The clearance in rats and cynos was higher (~2-fold) than that observed with dogs. The volume of distribution was the lowest in rat and moderate in dogs and cynos. The mean residence time and half-life were less than 1 h in all three species.

Table-7: Intravenous (IV) cassette dosing pharmacokinetics (PK) in rats

| Compd. | Microsome T _{1/2} min (h/r) | CL ml/min/kg | V _{ss} L/kg | AUC _{total} nM•h | t _{1/2} h |
|-----------|--|---------------------|-----------------------------|----------------------------------|---------------------------|
| 50 | 90, 70 | 4.0 | 0.24 | 4796 | 1.18 |
| 51 | 53, 67 | 10 | 0.22 | 2156 | 0.74 |
| 52 | 31, 7.5 | 23 | 0.18 | 624 | 0.35 |
| 53 | 40, 9.7 | 16 | 0.68 | 248 | 1.39 |
| 54 | >120, 45 | 64 | 0.81 | 183 | 0.25 |
| 55 | >120, 59 | 16 | 0.75 | 309 | 0.88 |

intravenous dosing solution 70%PEG400; 20%H₂O; 10%EtOH. CL = clearance, V_{ss} = steady-state volume of distribution, AUC = area under the curve, t_{1/2} = half life

Table-8: Multi species pharmacokinetic data for compound **55**.

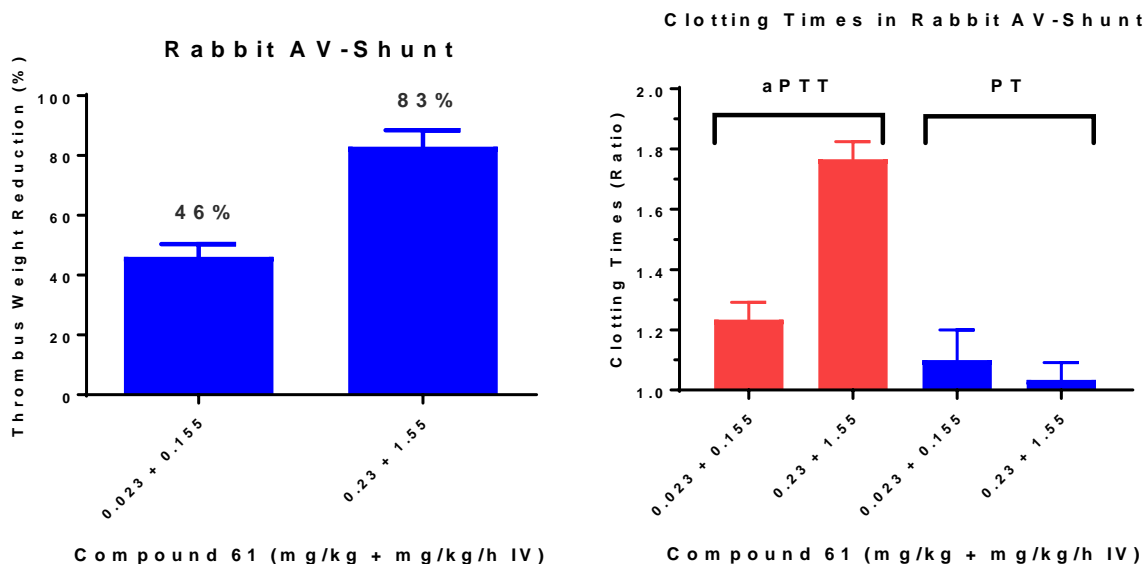
| Animal | Dose | CL | Vss | AUC _{total} | t _{1/2} |
|---------|-------|-----------|------|----------------------|------------------|
| Species | mg/kg | ml/min/kg | L/kg | nM•h | h |
| Rat | 0.5 | 31 | 0.32 | 441 | 0.22 |
| Rabbit | 0.5 | 43 | 0.71 | 270 | 0.6 |
| Dog | 4.75 | 15 | 1.02 | 7757 | 1.05 |
| Cyno | 2.03 | 31 | 1.16 | 1590 | 0.78 |

CL = clearance, Vss = steady-state volume of distribution, AUC = area under the curve, t_{1/2} = half life

IN VIVO EFFICACY IN THE RABBIT ARTERIOVENOUS SHUNT MODEL

Compound **55** was next advanced into the rabbit arteriovenous shunt (AV-shunt) thrombosis model^{11a} for efficacy determination. When evaluated in this model, compound **55** (rabbit FXIa Ki = 3 nM; rabbit activated plasma kallikrein Ki 1,100 nM) demonstrated a dose-response relationship with respect to inhibiting thrombus formation (Figure-9). At the highest dose evaluated (0.23 + 1.55 mg/kg/h IV), the compound showed an 83 % inhibition of thrombus formation and increased aPTT up to 1.8-fold over baseline, with no prothrombin time (PT) changes noted. Changes in aPTT but not PT are consistent with the mechanism of inhibiting FXIa. Compound **55** was evaluated in a rabbit cuticle bleeding model,^{11b} at twice the dose used in the AV-shunt model (0.46 mg/kg+3.1 mg/kg/h) and did not increase the bleeding time as compared to vehicle. The combination of aspirin (4 mg/kg/h IV) and **55** (0.46 mg/kg+3.1 mg/kg/h) resulted in bleeding times that were not greater than for aspirin treatment alone.^{12a}

Figure-9. Antithrombotic and clotting effects (aPTT and PT) of Compound **55** in the rabbit AV-Shunt model. Data are means ± SEM (n = 3 per group).



ADDITIONAL PROFILE FOR COMPOUND 55

The protease selectivity profile for compound **55** is shown in Table-11. The compound is a highly potent FXIa inhibitor (FXIa $K_i = 0.7$ nM) with an excellent protease selectivity profile.

The aqueous solubility for compound **55** was measured in buffer systems that would be clinically acceptable, and its long term solution stability was also evaluated. The crystalline form of **55**

Table-11. The human serine protease selectivity profile for **55**.

| Human Enzyme K_i (nM) ^a | 55 |
|--------------------------------------|-----------|
| Factor XIa | 0.71 |
| Factor VIIa ^b | >13,000 |
| Factor IXa | >27,000 |
| Factor Xa ^b | >9,000 |
| Factor XIIa | >3,000 |
| Plasma kallikrein | 310 |
| Tissue kallikrein-1 | >10,000 |
| Thrombin ^b | >13,000 |

| | |
|----------------------|---------|
| Trypsin ^b | >6,200 |
| Activated Protein C | >21,000 |
| Plasmin | >25,000 |
| TPA | >6,200 |
| Urokinase | >15,000 |
| Chymotrypsin | 11,000 |

^aK_i values in nM were obtained using human purified enzymes at 37 °C. ^bK_i values in nM were obtained using human purified enzymes at 25 °C.

(hemi-hydrate) showed good aqueous solubility (Table-9), and it had good stability for over 90 days and at varying temperatures (Table-10). The measured pK_a values for **55** were 4.7 and 4.1 for the N-Me-piperazine and carboxylic acid groups, respectively. The free fraction for **55** in human, rat, dog and cynomolgus monkey serum was 33.2 %, 44.8 %, 67.5 % and 51.8 %, respectively. The compound also showed no CYP activity (IC₅₀ values > 40 μM) and was stable in human, rat and dog liver microsomes (T_{1/2} = 108, 59, 120 min, respectively). Compound **55** was AMES negative.

Table-9: Pharmaceutical properties for compound **55**

| | | |
|-----------------------------------|------------------|--------------------|
| pK _a Acid (a) Base (b) | 4.1 (a); 4.7 (b) | |
| HPLC Log D | 1.40 | |
| Aqueous Solubility | pH | Solubility (mg/mL) |
| | 6.7 | 0.26 |
| | 7.4 | 1.5 |
| | 8.0 | 11 |
| | 8.3 | >25 |
| | 8.5 | >100 |

Table-10: Buffer-pH-temperature solution stability for **55** after 90 days

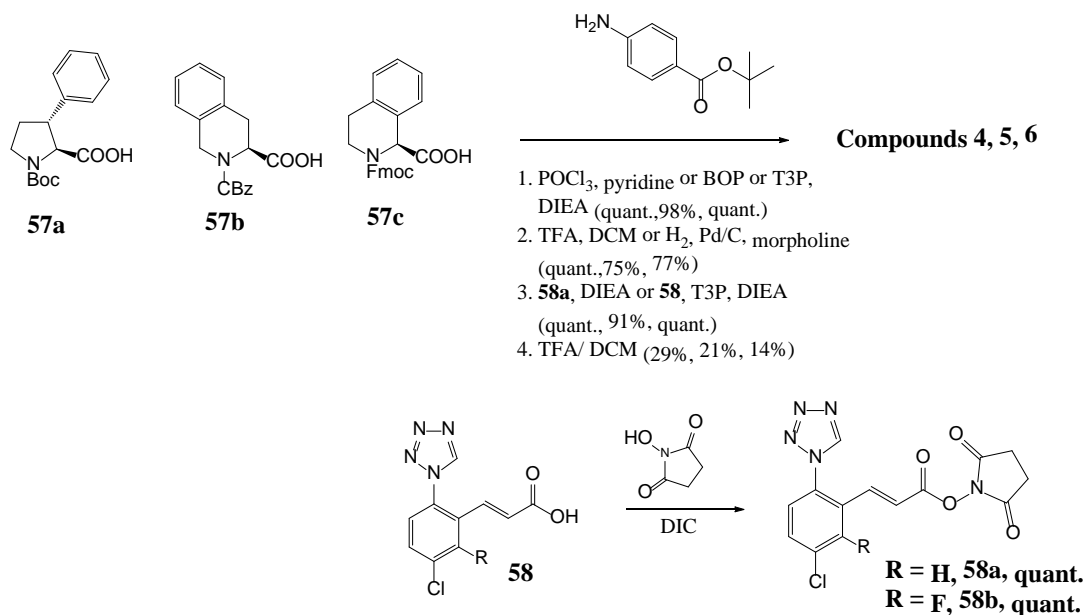
| Buffers | pH | 25 °C | 37 °C | 50 °C |
|-----------------|-----|--------|--------|--------|
| 0.1 M Phosphate | 6.5 | 99.9 % | 99.8 % | 95.4 % |
| 0.1 M Phosphate | 7.4 | 100 % | 99.0 % | 94.6 % |

| | | | | |
|------------|-----|------|--------|------|
| 0.1 M Tris | 8.0 | 99 % | 99.7 % | 94 % |
|------------|-----|------|--------|------|

CHEMISTRY

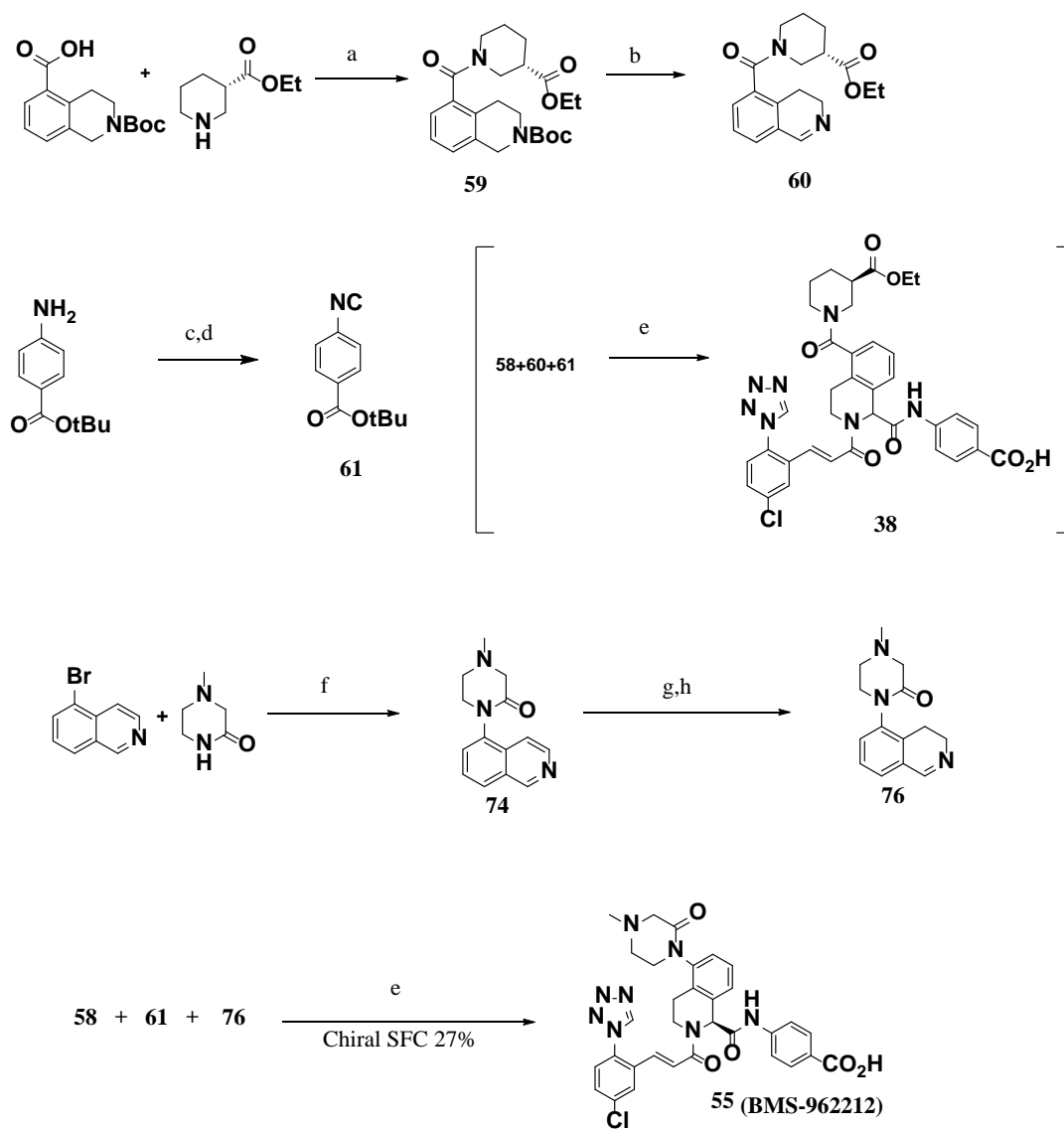
Compounds **4-6** were prepared in a three step sequence from commercially available materials **57a-c** (Scheme-1). Standard amide couplings of **57a-c** with BOP reagent and Hunig's base, followed by removal of the N-Boc protecting group and coupling with (*E*)-3-(5-chloro-2-(1*H*-tetrazol-1-yl)phenyl)acrylic acid **58** afforded compounds **4-6** in good overall yields. The highly elaborated THIQ scaffolds shown in Table-2 were accessed from commercially available starting materials which allowed rapid preparation of the final products via a three component Ugi reaction.^{10a,b} For example, compound **38** (Scheme-2) was prepared from commercially available 2-(*tert*-butoxycarbonyl)-1,2,3,4-tetrahydroisoquinoline-5-carboxylic acid. Coupling of this intermediate with (*S*)-ethyl-piperidine-3-carboxylate afforded compound **59** in good yield. To perform the Ugi reaction it was necessary to access the imine **60**. This was accomplished in a three step sequence by first removal of the Boc protecting group followed by neutralization and oxidation with excess activated MnO₂ in dichloromethane to provide **60** in 74% overall yield.

Scheme-1: Method for the preparation of compounds **4-6**.^a



Isonitrile intermediate **61** was prepared in two steps by heating *tert*-butyl-4-aminobenzoate in neat ethyl formate. The ensuing formamide intermediate was subsequently dehydrated to the isonitrile **61** by treatment with POCl₃ in THF containing TEA. The highly complex compounds were then assembled by the use of the three component Ugi reaction by combining intermediates **58**, **60** and **61** in EtOH. Treatment with TFA afforded compound **38** in low yield. The preparation of compound **55** required the availability of the imine intermediate **76**. This was easily obtained from commercially available 5-bromoisquinoline. Ullmann coupling of this material with *N*-methylpiperazinone in the presence of catalytic amount of CuI, 1,10-phenanthroline and K₂CO₃ at 130 °C in DMSO afforded the coupled intermediate **74** (31% yield). This was easily converted to the requisite imine intermediate **76** by hydrogenation with PtO₂ catalyst, followed by oxidation with excess MnO₂ in good overall yields. Ugi coupling of **76** with chlorophenyltetrazole

Scheme-2: The synthesis of compounds **38** and **55**.^a



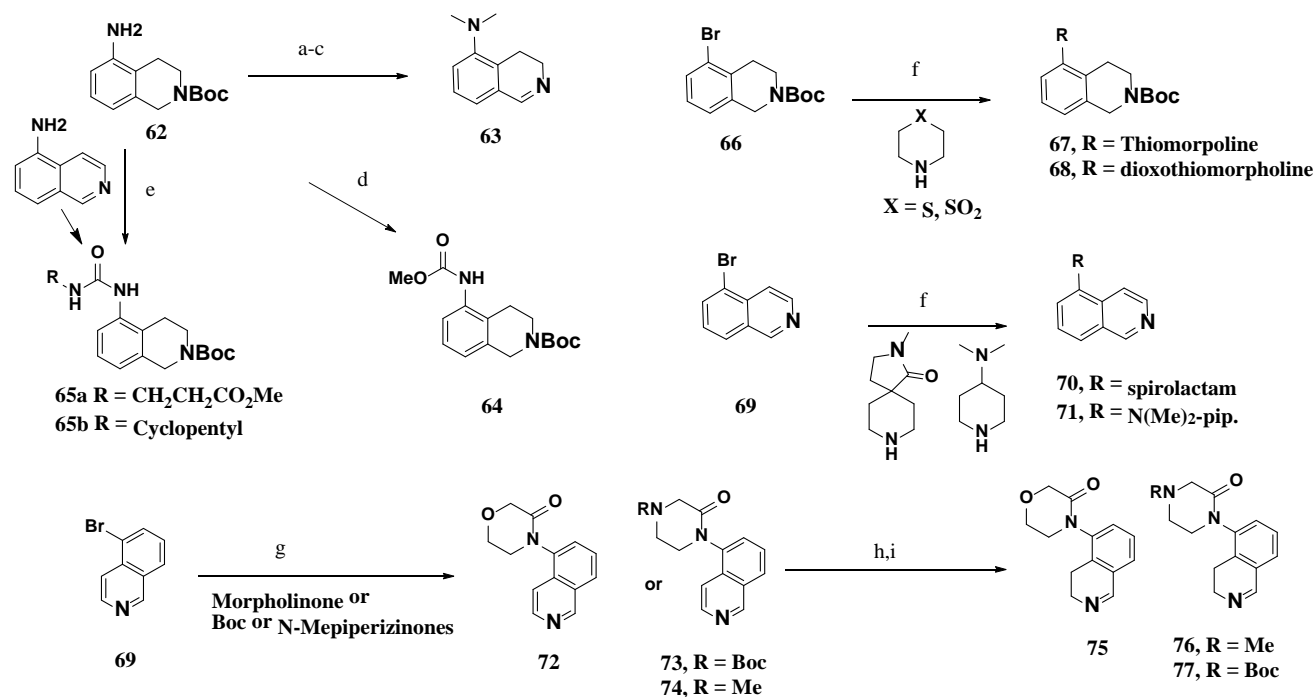
^a Reagents and conditions: (a) T3P, DIEA, EtOAc, 74%; (b) TFA, NaHCO₃, MnO₂ DCM 74% 3 steps; (c) Ethylformate reflux, >80% (d) POCl₃, TEA, THF 78% 2 steps; (e) Ugi Rxn. EtOH, 63°C, TFA 6% 2 steps; (f) CuI, DMSO, 1,10 phenanthroline, K₂CO₃, 130 °C, 31%; (g) PtO₂, H₂, EtOH, quant.; (h) MnO₂, DCM, 89%.

intermediate **58b** and isonitrile intermediate **61** in ethanol afforded **55** as a racemate in 33% yield.

Removal of the t-butyl ester with TFA, followed by chiral SFC separation, afforded the homochiral compound **55** in 27% yield. The Ugi methodology provided us with a unique opportunity to rapidly access multiple THIQ FXIa compounds. Homochiral compounds were separated by chiral SFC methods of the racemic Ugi coupled products and then deprotected with TFA to afford the desired analogs. Various imine intermediates that were employed in the Ugi methodology were easily

accessed using the methods outlined in Scheme-3. Commercially available *tert*-butyl 5-amino-3,4-dihydroisoquinoline-2(1*H*)-carboxylate **62** was readily converted to the dimethylamino compound **63**, the carbamate **64** or the urea intermediates **65a,b**. Buchwald-Hartwig C-N bond-forming reactions afforded intermediates **67-71** from commercially available bromides **66** and **69**, and Ullmann coupling provided access to intermediates **72-74** from **69**. Quinoline intermediates were hydrogenated to the corresponding THIQ intermediates and subsequently oxidized with MnO₂ to the respective imines **75-77** which were used as is in the Ugi coupling step to afford the elaborated racemic FXIa THIQ compounds as shown in Scheme-2..

Scheme-3: Schematic for the preparation of 5-amino substituted isoquinoline intermediates^a

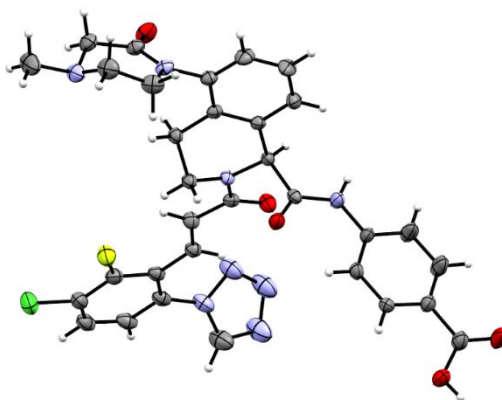


^aReagents and conditions: (a) NaH, MeI, THF, 74%; (b) TFA, DCM; (c) MnO₂, DCM, 55% 2 steps; (d) MeCO₂Cl, NaOH, DCM, 95%; (e) isocyanate, Hunig's base, DCM, **65a** 95%, **65b** 90%; (f) NaOtBu, BINAP, Pd₂(dba)₃, toluene, 130 °C, **67** 98%, **68** 83%, **70** 80%, **71** 89%; (g) K₂CO₃, 1,10-phenanthroline, CuI, DMSO, 130 °C 24h, **72** 82%, **73** 80%, **74** 31%; (h) PtO₂, EtOH, [H] 55psi; (i) MnO₂, DCM, **75** 83%, **76** 28%, **77** 65%.

SINGLE CRYSTAL X-RAY STRUCTURE FOR COMPOUND 55

A single crystal x-ray structure of compound **55** was obtained to confirm the absolute stereochemistry at the THIQ chiral center to be (*S*). This is similar to the energetically more favorable bound conformation seen for a number of our THIQ analogs. The overall x-ray structure for **55** is similar to its FXIa model structure shown in Figure-8b.

Figure-11: Single crystal x-ray for compound **55**.



Crystal data. (CCDC 1568523), C₃₂H₂₈ClFN₈O₅·0.5H₂O, MW = 668.08, orthorhombic I₂12₁2₁, *a* = 13.6547(3) Å, *b* = 18.7590(3) Å, *c* = 24.7370(5) Å, *V* = 6336.3(2) Å³, *T* = 296(2) K, Cu-Kα, 19192 reflections, 3372 unique (*R*_{int} = 0.0364). *R*₁ = 0.0295, *wR*₂ = 0.0790 (for 3372 observed reflections with *I* > 2σ(*I*) and 430 parameters).

CONCLUSION

To identify a parenteral FXIa agent, we optimized FXIa affinity, in vitro anticoagulant activity, and aqueous solubility and targeted a pharmacokinetic profile suitable for acute antithrombotic therapy. The phenylalanine scaffold was used as a starting point to achieve these goals. Towards this end, proline and tetrahydroisoquinoline THIQ analogs **4** and **6** were prepared, both of which showed modest FXIa activity. The FXIa bound x-ray structure for the THIQ analog **6** showed that it bound to the active site in a similar manner to that observed for the phenylalanine compound **2**. The THIQ scaffold maintains the disulfide S2' interaction and also appears to form an edge-to-face interaction with His 57. Additional potency was achieved via substitution at the 5-position of

the THIQ, whereas substitution at the 6-8 THIQ positions was not tolerated due to the close proximity to the enzyme residues at the S2. Both electron withdrawing and donating groups were tolerated at the 5-position of the THIQ. The carboxamide P2 group appears to engage the water network in the S2 pocket. Various nitrogen based P2 analogs also demonstrated potent FXIa inhibitory activity and good clotting activity. Zwitterionic compounds had the best profile in terms of potency and in vitro anticoagulant activity as assessed by the in vitro aPTT assay. However, these analogs had low aqueous solubility at near physiological pH. The lactam P2 containing compounds had good FXIa potency, however solubility at pH 6.5 was modest preventing advancement. The potent and selective N-methylpiperazinone compound **55** demonstrated an acceptable solubility profile. Overall, compound **55** met the criteria suitable for advancement as a parenteral agent, including potent FXIa binding affinity, good anticoagulant activity both in vitro and in vivo, aqueous solubility, a pharmacokinetic profile with short half-life, and no off-target activity, and was advanced into development. As has recently been reported, **BMS-962212** has completed Phase 1 clinical trials (NCT03197779).^{12a,b}

EXPERIMENTAL SECTION

Experimental compounds: All reactions were carried out using commercial grade reagents and solvents. NMR chemical shifts (δ) are reported in parts per million (ppm) relative to internal TMS. Normal phase chromatography was carried out on ISCO CombiFlash[®] systems using prepacked silica cartridges and eluted with gradients of the specified solvents. Preparative reverse phase high pressure liquid chromatography (HPLC) was carried out on C18 HPLC columns using methanol/water gradients containing 0.1 % trifluoroacetic acid unless otherwise stated. Deprotection with TFA followed by re-purification using standard reverse phase conditions afforded the desired homochiral compounds. Homochiral compounds were separated from racemic

1
2
3 *t*-butyl ester analogs using chiral SFC method on a Chiralpak AD-H column, 250 x 30 mm, 5 μ m,
4
5 using 60% of ethanol and isopropanol mixture (1:1), 40 % CO₂ with 0.1 % diethylamine modifier
6
7 at a flow rate of 90 ml/min, at 150 bar BP, 35 °C. The desired (*S*) homochiral compounds were
8
9 obtained as the second eluting enantiomer via this methodology. Purity of all final compounds was
10
11 determined by analytical HPLC using the following conditions: SunFire C18 column (3.5 μ m C18,
12
13 3.0 x 150 mm); Gradient elution (0.5 mL / min) from 10-100% Solvent B for 12 min and then
14
15 100% Solvent B for 3 min. Solvent A is (95% water, 5 % acetonitrile, 0.05 % TFA) and Solvent
16
17 B is (5% water, 95% acetonitrile, 0.05% TFA); monitoring UV absorbance at 220 and 254 nm.
18
19 Using this methodology the final compounds were >95% pure with HPLC retention times (*t_R*)
20
21 recorded. Final compounds that contained basic functionalities were typically isolated as
22
23 trifluoroacetic acid salts following HPLC purifications.
24
25
26
27
28
29

30 **4-((2*S*,3*R*)-1-((*E*)-3-(5-Chloro-2-(1*H*-tetrazol-1-yl)phenyl)acryloyl)-3-phenylpyrrolidine-2-**
31 **carboximidamido)benzoic acid (4).** *Step 1.* (2*S*,3*R*)-1-(*tert*-butoxycarbonyl)-3-
32 phenylpyrrolidine-2-carboxylic acid (0.15 g, 0.50 mmol) was dissolved in DCM (5 mL). To this
33
34 solution was added *tert*-butyl 4-aminobenzoate (0.10 g, 0.50 mmol), followed by pyridine (1 mL).
35
36 The reaction mixture was cooled to 0 °C, and to the solution was added POCl₃ (0.050 mL). The
37
38 reaction was stirred cold for 1 h and quenched with aqueous 1N HCl. The solution was extracted
39
40 with EtOAc (2 x 25 mL), dried (MgSO₄), filtered and evaporated to an oily mass. Purification via
41
42 an ISCO[®] column (4g) using hexane/EtOAc as eluents afforded 4-((2*S*,3*R*)-1-(*tert*-
43
44 butoxycarbonyl)-3-phenylpyrrolidine-2-carboxamido)benzoic acid (0.24 g, quant.). ¹H NMR
45
46 (CDCl₃) δ 7.79 (bs, 1H), 7.25-7.12 (m, 5H), 3.60-3.49 (m, 1H), 1.53 (s, 2H), 1.18-1.15(m, 4H).
47
48
49
50
51
52
53
54 LCMS *m/z*: 467.5 [M+H].⁺
55
56
57
58
59
60

Step 2. The product obtained from Step 1 was dissolved in DCM (5 mL) and cooled to 0 °C. To this solution was added TFA (0.5 mL), and the reaction was warmed to rt for 2 h. After this time, the solution was concentrated to give a pinkish solid mass which was redissolved in DMF (10 mL), and to this solution was added tetrazole intermediate **58b** (0.22 g, 0.64 mmol) followed by TEA (1.0 mL). The reaction mixture was stirred at rt overnight. The reaction was then quenched with water (50 mL) and acidified with 1N HCl. The solution was extracted with EtOAc (2 x 25 mL), dried (MgSO₄), filtered and concentrated. The crude material was purified by reverse phase HPLC. The pure fractions were collected and lyophilized to afford compound **4** (0.10 g, 29%) as a white solid. ¹H NMR (DMSO-d₆) δ 9.74(s, 1H), 8.35(s, 1H), 7.30(m, 2H), 7.22-7.57(m, 5H), 7.35-7.18(m, 5H), 6.85(d, 2H), 4.50(d, 1H), 3.98(m, 2H), 3.85(m, 2H), 2.40(m, 1H). LCMS m/z: 543.5 [M+H].⁺ HPLC purity > 95%, HPLC t_R = 5.59 min.

(S,E)-4-(2-(3-(5-Chloro-2-(1H-tetrazol-1-yl)phenyl)acryloyl)-1,2,3,4-tetrahydroisoquinoline-3-carboxamido)benzoic acid (5). Step 1. To (S)-2-((benzyloxy)carbonyl)-1,2,3,4-

tetrahydroisoquinoline-3-carboxylic acid, (**57b**) (0.16 g, 0.52 mmol) in pyridine (2 mL), was added *tert*-butyl-4-aminobenzoate (0.10 g, 0.52 mmol), and the reaction mixture was then cooled to 0 °C. POCl₃ (0.050 mL, 0.52 mmol) was carefully added dropwise to the cold solution. After 1 h, the reaction was partitioned between water (15 mL) and EtOAc (40 mL). The organic layer was washed with aqueous 0.1N HCl (10 mL) and brine (10 mL), and dried over MgSO₄.

Purification by silica gel chromatography (DCM/MeOH) afforded (S)-benzyl 3-(4-(*tert*-butoxycarbonyl)phenylcarbamoyl)-3,4-dihydroisoquinoline-2(1H)-carboxylate (0.25 g, 98 %) as a white solid. ¹H NMR (400 MHz, CDCl₃) δ 7.96 (d, *J*=8.59 Hz, 1 H), 7.80 (d, *J*=8.59 Hz, 2 H), 7.45-7.20 (m, 10 H), 5.25 (s, 2 H), 4.75- 4.65 (m, 2 H), 4.45 (m, 1 H), 3.69 (m, 1 H), 3.34 (m, 1 H), 1.60 (s, 9 H), LCMS (ESI) m/z: 487.4 [M+H].⁺

Step 2. (S)-Benzyl 3-(4-(*tert*-butoxycarbonyl)phenylcarbamoyl)-3,4-dihydroisoquinoline-2(1*H*)-carboxylate (0.25 g, 0.50 mmol) was hydrogenated at 50 psi for 1 h in EtOH (25 mL) over 10% Pd/C (35 mg). After this time, the reaction mixture was filtered through Celite[®] and concentrated to give (S)-*tert*-butyl 4-(1,2,3,4-tetrahydroisoquinoline-3-carboxamido)benzoate (0.13 g, 75%) as a pale grey solid. ¹H NMR (400 MHz, CDCl₃) δ 9.55 (s, 1 H), 7.96 (d, *J*=8.59 Hz, 2 H), 7.67 (d, *J*=8.59 Hz, 2 H), 7.16 - 7.24 (m, 3 H), 7.06 - 7.13 (m, 1 H), 4.00 - 4.12 (m, 2 H), 3.69 (dd, *J*=10.48, 5.43 Hz, 1 H), 3.34 (dd, *J*=16.29, 5.43 Hz, 1 H), 2.92 (dd, *J*=16.42, 10.36 Hz, 1 H), 1.69 - 1.75 (m, 1 H), 1.60 (s, 9 H). LCMS (ESI) *m/z*: 353.4 [M+H].⁺

Step 3. (S)-*tert*-Butyl 4-(1,2,3,4-tetrahydroisoquinoline-3-carboxamido)benzoate (0.10 g, 0.28 mmol) was dissolved in DMF (2 mL), and to this solution was added **58a** (99 mg, 0.28 mmol), followed by the addition of DIEA (0.15 mL, 0.85 mmol). The reaction was stirred at rt for 1 h, quenched with water (10 mL) and extracted with EtOAc (3 x 20 mL). The combined organic layers were washed with water (10 mL) and brine (10 mL), and dried over MgSO₄. The crude material was purified by silica gel column chromatography to afford (S,*E*)-*tert*-butyl 4-(2-(3-(5-chloro-2-(1*H*-tetrazol-1-yl)phenyl)acryloyl)-1,2,3,4-tetrahydroisoquinoline-3-carboxamido)benzoate (0.15 g, 91 %) as a yellow solid. ¹H NMR (400 MHz, DMSO-*d*₆) δ 10.37 (s, 1H), 9.88 (s, 1H), 8.49 (d, *J*=2.2 Hz, 1H), 7.93 - 7.79 (m, 3H), 7.79 - 7.72 (m, 2H), 7.66 (t, *J*=4.4 Hz, 1H), 7.65 - 7.60 (m, 2H), 7.31 - 7.13 (m, 3H), 6.97 (d, *J*=15.2 Hz, 1H), 5.14 (d, *J*=15.4 Hz, 1H), 5.02 (t, *J*=5.9 Hz, 1H), 4.88 (d, *J*=15.4 Hz, 1H), 3.34 - 3.23 (m, 1H), 3.22 - 3.09 (m, 1H), 1.54 (s, 9H). LCMS (ESI) *m/z*: 585.2 [M+H].⁺

Step 4. (S,*E*)-*tert*-Butyl 4-(2-(3-(5-chloro-2-(1*H*-tetrazol-1-yl)phenyl)acryloyl)-1,2,3,4-tetrahydroisoquinoline-3-carboxamido)benzoate (0.15 g, 0.25 mmol) was dissolved in DCM (5 mL), and to this solution was added TFA (2 mL). After 3 h, the reaction was concentrated and

purified by reverse phase HPLC, and the collected pure fraction lyophilized to afford **5** (32 mg, 21 %) as a pale yellow solid. ¹H NMR (400 MHz, CD₃OD) δ 9.55 (s, 1 H), 8.28 (d, *J*=2.02 Hz, 1 H), 7.94 (d, *J* = 8.59 Hz, 2 H), 7.65 - 7.74 (m, 1 H), 7.55 - 7.63 (m, 3 H), 7.44 (d, *J*=15.41 Hz, 1 H), 7.36 (d, *J*=4.55 Hz, 1 H), 7.22 - 7.29 (m, 3 H), 7.20 (d, *J*=15.41 Hz, 1 H), 4.96 - 5.08 (m, 2 H), 4.88 - 4.91 (m, 1 H), 3.23 - 3.37 (m, 2 H). LCMS (ESI) *m/z*: 529.0 [M+H]⁺ HPLC purity > 95%. HPLC *t_R* = 8.5 min.

(*S,E*)-4-(2-(3-(5-Chloro-2-(1*H*-tetrazol-1-yl)phenyl)acryloyl)-1,2,3,4-tetrahydroisoquinoline-1-carboxamido)benzoic acid (6**).** *Step 1.* To (*S*)-2-(((9*H*-fluoren-9-yl)methoxy)carbonyl)-1,2,3,4-tetrahydroisoquinoline-3-carboxylic acid (**57c**) (0.36 g, 0.89 mmol) in EtOAc (2 mL), was added *tert*-butyl 4-aminobenzoate (0.19 g, 0.99 mmol), and the reaction mixture was cooled in an ice bath. To the cooled solution was added DIEA (0.47 mL, 2.7 mmol) and T3P (50 % in EtOAc, 0.50 mL, 1.8 mmol). After 1 h, the reaction was partitioned with water (15 mL) and ethyl acetate (40 mL). The organic layer was washed with aqueous 0.1N HCl (10 mL) and brine (10 mL), dried (MgSO₄), filtered and concentrated to afford (*S*)-(9*H*-fluoren-9-yl)methyl 1-(4-(*tert*-butoxycarbonyl)phenylcarbamoyl)-3,4-dihydroisoquinoline-2(1*H*)-carboxylate (0.64 g) as a white solid. ¹H NMR (400 MHz, CDCl₃) δ 9.08 (br s, 1H), 7.93 - 7.86 (m, 3H), 7.84 - 7.77 (m, 1H), 7.67 - 7.59 (m, 2H), 7.56 - 7.50 (m, 1H), 7.46 - 7.37 (m, 2H), 7.37 - 7.21 (m, 7H), 5.77 (br s, 1H), 4.59 (br s, 2H), 4.33 (br t, *J*=6.7 Hz, 1H), 3.82 (br d, *J*=4.2 Hz, 2H), 3.24 - 3.02 (m, 1H), 2.95 - 2.66 (m, 1H), 1.61 (s, 9H). LCMS (ESI) *m/z*: 575.4 [M+H]⁺

Step 2. (*S*)-(9*H*-Fluoren-9-yl)methyl-1-(4-(*tert*-butoxycarbonyl)phenylcarbamoyl)-3,4-dihydroisoquinoline-2(1*H*)-carboxylate (0.64 g, 1.1 mmol) was dissolved in DMF (4 mL), and morpholine (0.30 mL) was added to this solution. After 30 min., the reaction was partitioned with water (10 mL) and ethyl acetate (20 mL). The organic layer was washed with water (10 mL) and

brine (10 mL), dried (MgSO₄), filtered and concentrated to afford (*S*)-*tert*-butyl 4-(1,2,3,4-tetrahydroisoquinoline-1-carboxamido)benzoate (0.30 g, 77%) as a white foam. A sample of (*S*)-*tert*-butyl 4-(1,2,3,4-tetrahydroisoquinoline-1-carboxamido)benzoate was purified by reverse phase HPLC. ¹H NMR (400 MHz, CD₃OD) δ 7.98 - 7.81 (m, 2H), 7.76 - 7.60 (m, 2H), 7.35 (d, *J*=7.3 Hz, 1H), 7.32 - 7.19 (m, 3H), 5.17 (s, 1H), 3.75 (dt, *J*=12.5, 5.7 Hz, 1H), 3.43 (ddd, *J*=12.5, 8.7, 5.6 Hz, 1H), 3.17 - 3.08 (m, 1H), 3.08 - 2.91 (m, 1H), 1.49 (s, 9H). LCMS (ESI) *m/z*: 353.5 [M+H].⁺

Step 3. Compound **58a** (0.21 g, 0.85 mmol) and (*S*)-*tert*-butyl 4-(1,2,3,4-tetrahydroisoquinoline-1-carboxamido)benzoate (0.30 g, 0.85 mmol) were dissolved in DMF (5 mL) and cooled in ice bath. To this mixture was added DIEA (0.45 mL, 2.5 mmol) and T3P (50 % in EtOAc, 0.48 mL, 1.7 mmol). After 1 h, the reaction was quenched with water (50 mL), extracted with EtOAc (2 x 50 mL), dried with MgSO₄, filtered and concentrated to afford crude (*S,E*)-*tert*-butyl 4-(2-(3-(5-chloro-2-(1*H*-tetrazol-1-yl)phenyl)acryloyl)-1,2,3,4-tetrahydroisoquinoline-1-carboxamido)-benzoate as a yellow oil that was carried onto the next step. LCMS (ESI) *m/z*: 585.3 [M+H].⁺

Step 6. The crude (*S,E*)-*tert*-butyl 4-(2-(3-(5-chloro-2-(1*H*-tetrazol-1-yl)phenyl)acryloyl)-1,2,3,4-tetrahydroisoquinoline-1-carboxamido)benzoate was dissolved in DCM (15 mL), and to this solution was added TFA (2 mL). The reaction mixture was stirred at rt for 1 h. The reaction was concentrated, and the residue purified by reverse phase HPLC and lyophilized to afford **6** (62 mg, 14 %) as a white solid. ¹H NMR (400 MHz, DMSO-*d*₆) δ 10.72 (1 H, s), 9.79 - 9.84 (1 H, m), 8.38 (1 H, d, *J*=2.02 Hz), 7.76 - 7.85 (2 H, m), 7.57 - 7.72 (5 H, m), 7.52 - 7.56 (1 H, m), 7.49 (1 H, d), 7.15 - 7.26 (3 H, m), 6.89 (1 H, d, *J*=15.16 Hz), 5.74 (1 H, s), 4.24 - 4.32 (1 H, m), 3.81 (1 H, ddd, *J*=12.44, 8.40, 4.17 Hz), 3.04 - 3.19 (1 H, m), 2.85 (1 H, td). LCMS (ESI) *m/z*: 529.2 [M+H].⁺ HPLC purity > 95%. HPLC: *t_R* = 10.4 min.

(E)-4-(6-(3-(5-Chloro-2-(1*H*-tetrazol-1-yl)phenyl)acryloyl)-5,6,7,8-tetrahydro-1,6-

naphthyridine-5-carboxamido)benzoic acid (7). *Step 1.* 3-Bromo-5,6,7,8-tetrahydro-1,6-naphthyridine (0.50 g, 2.3 mmol) in EtOH (30 mL) was hydrogenated at 55 psi for 3.5 h with 10% Pd/C (40 mg). The reaction mixture was filtered through Celite® and concentrated to afford (0.31 g, 100%) of 5,6,7,8-tetrahydro-1,6-naphthyridine as a yellow solid. ¹H NMR (400 MHz, DMSO-*d*₆) δ 9.09 (1 H, br. s.), 8.48 (1 H, d, *J*=3.3 Hz), 7.67 (1 H, d, *J*=7.6 Hz), 7.31 (1 H, dd, *J*=7.7, 4.7 Hz), 4.34 (2 H, s), 3.52 (2 H, t, *J*=6.3 Hz), 3.10 (2 H, t, *J*=6.3 Hz). LCMS (ESI) *m/z*: 135.0 [M+H].⁺

Step 2. To 5,6,7,8-tetrahydro-1,6-naphthyridine (0.31 g, 2.3 mmol) in a mixture of DCM (50 mL)/DMSO (0.5 mL) was added MnO₂ (3.7 g, 42 mmol), and the reaction was stirred for 24 h at rt. The reaction mixture was filtered through Celite® and concentrated to afford 7,8-dihydro-1,6-naphthyridine (0.31 g, quant.) as a yellow solid which was used directly in the next step. ¹H NMR (400 MHz, DMSO-*d*₆) δ 8.51 (1 H, dd, *J*=4.9, 1.6 Hz), 8.38 (1 H, t, *J*=2.3 Hz), 7.79 (1 H, dd, *J*=7.6, 1.8 Hz), 7.37 (1 H, dd, *J*=7.5, 4.9 Hz), 3.78 - 3.91 (2 H, m), 2.79 - 2.89 (2 H, m). LCMS (ESI) *m/z*: 133.0 [M+H].⁺

Step 3. In a small vial 7,8-dihydro-1,6-naphthyridine (50 mg, 0.38 mmol), **61** (77 mg, 0.38 mmol) and **58** (95 mg, 0.38 mmol) were combined in MeOH (6 mL). The sealed reaction mixture was heated to 55 °C for 72 h. The reaction was cooled and concentrated, and the residue was partitioned with sat'd NaHCO₃ (10 mL) and EtOAc (30 mL). The organic layer was washed with brine (10 mL) and dried (MgSO₄). After filtration and concentration, the crude product was treated with 50% TFA/DCM (5 mL) for 1 h, then concentrated, and the residue was purified by reverse phase HPLC and lyophilized to afford **7** (32 mg, 13 %) as a tan solid. ¹H NMR (400 MHz, CD₃OD) δ 9.52 (1 H, s), 8.72 (1 H, d, *J*=5.6 Hz), 8.54 (1 H, d, *J*=8.1 Hz), 8.19 (1 H, s), 7.93 (2 H, d, *J*=8.3 Hz), 7.85 - 7.92 (1 H, m), 7.62 - 7.69 (3 H, m), 7.54 - 7.59 (1 H, m), 7.42 (1 H, d, *J*=15.2 Hz), 7.22

- 7.28 (1 H, m), 6.29 (1 H, s), 4.46 (1 H, dd, $J=8.7, 4.9$ Hz), 4.11 - 4.29 (1 H, m), 3.44 (2 H, br. s.).

LCMS (ESI) m/z : 530.2 $[M+H]^+$ HPLC purity > 95%. HPLC: t_R = 4.70 min.

(*E*)-4-(2-(3-(5-Chloro-2-(1*H*-tetrazol-1-yl)phenyl)acryloyl)-1,2,3,4-tetrahydro-2,7-

naphthyridine-1tetrahydroisoquinoline-3-carboxamido)benzoic acid (8). The title compound

was prepared as described for compound 7. ^1H NMR (400 MHz, CD_3OD) δ 9.53 (1 H, s), 8.79 (1

H, s), 8.55 (1 H, br. s.), 8.21 (1 H, d, $J=1.8$ Hz), 7.97 (2 H, d, $J=8.6$ Hz), 7.52 - 7.72 (4 H, d,

$J=15.6$ Hz), 7.32 - 7.42 (1 H, m), 7.20 - 7.31 (1 H, d, $J=15.4$ Hz), 6.19 (1 H, s), 4.16 (1 H, br. s.),

2.56 - 2.98 (4 H, m). LCMS (ESI) m/z : 529.9 $[M+H]^+$ HPLC purity > 95%. HPLC: t_R = 4.71

min.

(*E*)-4-(5-(3-(5-chloro-2-(1*H*-tetrazol-1-yl)phenyl)acryloyl)-4,5,6,7-tetrahydro-1*H*-

pyrazolo(4,3-*c*)pyridine-4-carboxamido)benzoic acid (9). The title compound was prepared as

described for compound 7. ^1H NMR (400 MHz, $\text{DMSO}-d_6$) δ 12.48 - 12.85 (1 H, m), 10.68 (1

H, s), 9.87 (1 H, s), 8.49 (1 H, d, $J=2.0$ Hz), 7.86 - 7.97 (2 H, m), 7.65 - 7.81 (5 H, m), 7.63 (1 H,

d, $J=3.3$ Hz), 6.95 (1 H, d, $J=15.2$ Hz), 5.89 (1 H, s), 4.53 - 4.68 (1 H, m), 3.76 - 3.94 (1 H, m),

2.92 - 3.14 (1 H, m), 2.77 - 2.87 (2 H, m). LCMS (ESI) m/z : 519.1 $[M+H]^+$ HPLC purity > 95%.

HPLC: t_R = 5.62 min.

(*E*)-4-(5-(3-(5-chloro-2-(1*H*-tetrazol-1-yl)phenyl)acryloyl)-2-methyl-4,5,6,7-tetrahydro-2*H*-

pyrazolo(4,3-*c*)pyridine-4-carboxamido)benzoic acid (10). *Step 1.* To a solution of *tert*-butyl

4-oxopiperidine-1-carboxylate (2 g, 10 mmol) in ethanol (2 mL), was added methylhydrazine

sulfate (2.2 g, 15 mmol) and potassium carbonate (2.5 g, 18 mmol). The reaction mixture was

heated to reflux for 12 h, then cooled and concentrated to dryness to afford crude *tert*-butyl 4-(2-

methylhydrazono) piperidine-1-carboxylate (2.3 g, quant.), which was carried onto the next step.

¹H NMR (400 MHz, CD₃OD) δ 3.48 - 3.57 (4 H, m), 3.3 (3 H, s), 2.38 (4 H, t, *J*=8.0 Hz), 1.46 (9 H, s).

Step 2. *tert*-Butyl 4-(2-methylhydrazono) piperidine-1-carboxylate (0.50 g, 2.2 mmol) was stirred in a solution of DMF-DMA (2.5 mL) and DMF (2.5 mL) and heated to 90 °C for 12 h. The reaction was concentrated to dryness and purified by column chromatography to afford *tert*-butyl 2-methyl-6,7-dihydro-2*H*-pyrazolo(4,3-*c*)pyridine-5(4*H*)-carboxylate (0.40 g, 77%) as a pale yellow oil. LCMS (ESI) *m/z*: 238.2 [*M*+*H*].⁺

Step 3. To a cold (0 °C) solution of *tert*-butyl 2-methyl-6,7-dihydro-2*H*-pyrazolo(4,3-*c*)pyridine-5(4*H*)-carboxylate (0.23 g, 0.97 mmol) in dioxane (5 mL) was added 4 M HCl in dioxane (2 mL). After stirring for 18 h the reaction was concentrated. The crude material was dissolved in water (25 mL), and the organic layer was extracted with EtOAc (4 x 20 mL), dried over Na₂SO₄, filtered and concentrated to afford 2-methyl-4, 5, 6, 7-tetrahydro-2*H*-pyrazolo(4,3-*c*)pyridine (120 mg, 91%) as a pale yellow solid. ¹H NMR (300 MHz, CDCl₃) δ 7.04 (1 H, s), 3.86 (5 H, d, *J*=9.0 Hz), 3.13 (2 H, t, *J*=6.0 Hz), 2.73 (2 H, t, *J*=6.0 Hz).

Step 4. 2-Methyl-4, 5, 6, 7-tetrahydro-2*H*-pyrazolo(4,3-*c*)pyridine (107 mg, 0.78 mmol) was oxidized as described for **7** to afford 2-methyl-6,7-dihydro-2*H*-pyrazolo(4,3-*c*)pyridine (80 mg, 76%). ¹H NMR (300 MHz, CDCl₃) δ 8.30 (1 H, s), 7.36 (1 H, s), 3.89 (3 H, s), 3.85 (2 H, d, *J*=6.0 Hz), 2.77 (2 H, t, *J*=9.0 Hz).

Step 5. The multicomponent Ugi reaction as described for **7** using 2-methyl-6,7-dihydro-2*H*-pyrazolo(4,3-*c*)pyridine afforded **10**. ¹H NMR (400 MHz, DMSO-*d*₆) δ 12.77 (1 H, bs), 10.71 (1 H, s), 9.88 (1 H, s), 8.49 (1 H, s), 7.89 (2 H, d, *J*=8.0 Hz), 7.65 - 7.77 (6 H, m), 6.92 (1 H, d, *J*=15.2 Hz), 5.84 (1 H, s), 5.76 (3 H, s), 4.50 - 4.61 (2 H, m), 3.78 (4 H, s), 2.75 (2 H, s), 1.99 -

2.01 (1 H, m), 1.50 (2 H, d, $J = 7.2$ Hz). LCMS (ESI) m/z : 533.0 $[M+H]^+$ HPLC purity > 95%.

HPLC: $t_R = 8.66$ min.

(*E*)-4-(5-(3-(5-Chloro-2-(1*H*-tetrazol-1-yl)phenyl)acryloyl)-2-phenyl-4,5,6,7-tetrahydro-2*H*-pyrazolo(4,3-*c*)pyridine-4-carboxamido)benzoic acid (11). *Step 1.* To *tert*-butyl 4-oxopiperidine-1-carboxylate (10 g, 0.050 mmol) in DMF (50 mL) was added DMF-DMA (50 mL). The reaction was heated to reflux, and after 4 h, the solvents were removed. The residue was quenched with water, extracted with EtOAc (2 x 50 mL), dried over Na_2SO_4 , filtered and concentrated to afford (*E*)-*tert*-butyl 3-((dimethylamino)methylene)-4-oxopiperidine-1-carboxylate (11 g, 86%). LCMS (ESI) m/z : 255 $[M+H]^+$.

Step 2. To (*E*)-*tert*-butyl 3-((dimethylamino)methylene)-4-oxopiperidine-1-carboxylate (1.0 g, 4.9 mmol) in EtOH (20 mL) was added phenyl hydrazine (0.60 g, 5.8 mmol), and the reaction was heated to 80 °C for 6 h. The reaction mixture was concentrated and quenched with water, extracted with ethyl acetate (2 x 50 mL), washed with saturated $NaHCO_3$ solution (50 mL), water (50 mL), and brine (50 mL), dried over Na_2SO_4 , filtered and concentrated. The product was purified by silica gel column chromatography to afford *tert*-butyl 2-phenyl-6,7-dihydro 2*H*-pyrazolo(4,3-*c*)pyridine-5(4*H*)-carboxylate (0.4 g, 27%). LCMS (ESI) m/z : 300 $[M+H]^+$.

Step 3. To a cold (0 °C) solution of *tert*-butyl 2-phenyl-6,7-dihydro-2*H*-pyrazolo(4,3-*c*)pyridine-5(4*H*)-carboxylate (0.60 g, 0.20 mmol) in DCM (10 mL) was added HCl in dioxane (6 mL), and the reaction mixture was stirred for 5 h at rt. The reaction was concentrated and quenched with water, basified (1 N NaOH), and extracted with ethyl acetate (2 x 25 mL). The combined organics were washed with water (25 mL) and brine (25 mL), dried over Na_2SO_4 , and concentrated to afford 2-phenyl-4, 5, 6, 7-tetrahydro-2*H*-pyrazolo(4,3-*c*)pyridine (0.4 g, 100%). LCMS (ESI) m/z : 200 $[M+H]^+$.

Step 4. To a cold (0 °C) solution of 2-phenyl-4, 5, 6, 7-tetrahydro-2*H*-pyrazolo(4,3-*c*)pyridine (0.20 g, 1.0 mmol) in EtOH (2 mL) were added sodium acetate (0.16 g, 2.0 mmol) and iodine (0.50 g, 2.0 mmol). After 2 h at rt, the reaction mixture was quenched with water (25 mL) and then extracted with dichloromethane (2 x 25 mL). The collected organics were concentrated to afford 2-phenyl-6,7-dihydro-2*H*-pyrazolo(4,3-*c*)pyridine (0.15 g, 76%). LCMS (ESI) *m/z*: 198 [M+H].⁺

Step 5. The multicomponent Ugi reaction as described in **7** using 2-phenyl-6,7-dihydro-2*H*-pyrazolo(4,3-*c*)pyridine afforded **11**. ¹H NMR (400 MHz, DMSO-*d*₆) δ 12.7 (1 H, bs), 10.74 (1 H, s), 9.89 (1 H, s), 8.43 - 8.60 (2 H, m), 7.94 - 7.69 (9 H, m), 7.48 (2 H, t, *J*=7.6 Hz), 6.98 - 6.95 (2 H, m), 6.01 (1 H, s), 4.70 (1 H, d, *J*=14.8 Hz), 3.80 - 3.60 (1 H, m), 2.80 - 2.90 (2 H, m). LCMS (ESI) *m/z*: 595.2 [M+H].⁺ HPLC purity > 95%. HPLC: *t*_R = 9.92 min.

(*S,E*)-3-(2-(3-(5-Chloro-2-(1*H*-tetrazol-1-yl)phenyl)acryloyl)-1,2,3,4-tetrahydroisoquinoline-1-carboxamido)benzoic acid (16**).** Compound **16** was prepared in a similar manner as described for **6** starting with *tert*-butyl 3-aminobenzoate. ¹H NMR (400 MHz, CD₃OD) δ 9.55 (1 H, s), 8.18 - 8.23 (2 H, m), 7.74 - 7.82 (2 H, m), 7.66 - 7.71 (1 H, m), 7.53 - 7.62 (2 H, m), 7.38 - 7.45 (2 H, m), 7.33 - 7.37 (1 H, m), 7.27 - 7.33 (4 H, m), 7.17 - 7.25 (1 H, m), 5.84 (1 H, s), 4.33 (1 H, dt, *J*=12.06, 5.34 Hz), 3.82 - 3.89 (1 H, m), 2.92 - 3.03 (1 H, m). LCMS (ESI) *m/z*: 529.3 [M+H].⁺ HPLC purity > 95%. HPLC: *t*_R = 10.44 min.

(*S,E*)-Methyl 4-(2-(3-(5-chloro-2-(1*H*-tetrazol-1-yl)phenyl)acryloyl)-1,2,3,4-tetrahydroisoquinoline-1-carboxamido)phenylcarbamate (17**).** *Step 1.* To intermediate **57c** (0.25 g, 0.62 mmol) and 4-nitroaniline (95 mg, 0.69 mmol) in EtOAc (5 mL) was added T3P (50% in EtOAc, 0.26 mL, 0.93 mmol) and DIEA (0.32 mL, 1.8 mmol). After 24 h, the reaction was concentrated and purified by silica gel column chromatography to afford (*S*)-(9*H*-fluoren-9-

yl)methyl 1-(4-nitrophenylcarbamoyl)-3,4-dihydroisoquinoline-2(1*H*)-carboxylate (55 mg, 17%) as a bright yellow solid. LCMS (ESI) *m/z*: 520.4 [M+H].⁺

Step 2. (S)-(9*H*-fluoren-9-yl)methyl 1-(4-nitrophenylcarbamoyl)-3,4-dihydroisoquinoline-2(1*H*)-carboxylate (55 mg, 0.11 mmol) was stirred in a solution of acetone (8 mL) and water (3 mL). To this mixture was added zinc (0.20 g, 3.1 mmol), followed by ammonium chloride (0.33 g, 6.2 mmol). After 24 h, the reaction mixture was filtered and concentrated. The resulting concentrated solution was extracted with EtOAc (3 x 20 mL) and washed with brine (20 mL). The combined organic layers were dried over MgSO₄, filtered and concentrated to afford (S)-(9*H*-fluoren-9-yl)methyl 1-(4-aminophenylcarbamoyl)-3,4-dihydroisoquinoline-2(1*H*)-carboxylate (51 mg) which was carried onto the next step. LCMS (ESI) *m/z*: 490.3 [M+H].⁺

Step 3. To a mixture of DCM (3 mL) and pyridine (1 mL) was added (S)-(9*H*-fluoren-9-yl)methyl 1-(4-aminophenylcarbamoyl)-3,4-dihydroisoquinoline-2(1*H*)-carboxylate (51 mg, 0.11 mmol) and methyl chloroformate (0.048 mL, 0.62 mmol), and the reaction mixture was stirred for 30 min. The reaction was quenched with 1 N HCl, and the aqueous layer was extracted with DCM (3 x 20 mL), washed with brine (10 mL), dried (MgSO₄), filtered and concentrated to afford (S)-(9*H*-fluoren-9-yl)methyl 1-(4-(methoxycarbonylamino) phenylcarbamoyl)-3,4-dihydroiso-quinoline-2(1*H*)-carboxylate (57 mg) as a tan solid which was carried onto the next step. LCMS (ESI) *m/z*: 548.3 [M+H].⁺

Step 4. To (S)-(9*H*-fluoren-9-yl)methyl 1-(4-(methoxycarbonylamino)phenylcarbamoyl)-3,4-dihydroiso-quinoline-2(1*H*)-carboxylate (57 mg, 0.11 mmol) in DMF (1 mL) was added morpholine (0.30 mL). After 2 h, the reaction was partitioned with water (15 mL) and EtOAc (30 mL). The organic layer was washed with brine (10 mL), dried (MgSO₄) and concentrated to

afford (*S*)-methyl 4-(1,2,3,4-tetrahydroisoquinoline-1-carboxamido)phenylcarbamate (34 mg) which was used in next step without purification. LCMS (ESI) *m/z*: 326.4 [M+H].⁺

Step 5. Prepared **17** (5.0 mg, 19 %) in a similar manner as described for **6**. ¹H NMR (400 MHz, DMSO-*d*₆) δ 10.38 (1 H, s), 9.87 (1 H, s), 9.54 (1 H, s), 8.44 (1 H, d, *J*=2.27 Hz), 7.69 - 7.83 (2 H, m), 7.55 - 7.63 (1 H, m), 7.42 - 7.52 (2 H, m), 7.32 - 7.38 (2 H, m), 7.18 - 7.31 (4 H, m), 6.95 (1 H, d, *J*=15.41 Hz), 5.79 (1 H, s), 4.25 - 4.35 (1 H, m), 3.93 (1 H, s), 3.63 (3 H, s), 3.12 - 3.22 (1 H, m), 2.85 - 2.97 (1 H, m). LCMS (ESI) *m/z*: 558 [M+H].⁺ HPLC purity > 95%. HPLC: *t_R* = 8.08 min.

(*S,E*)-Methyl 4-(2-(3-(5-chloro-2-(1*H*-tetrazol-1-yl)phenyl)acryloyl)-1,2,3,4-tetrahydroisoquinoline-1-carboxamido)benzylcarbamate (18**).** Compound **18** (3.1 mg, 6.1%) was prepared in a similar manner as **17** and **6**. ¹H NMR (400 MHz, DMSO-*d*₆) δ 10.45 (1 H, s), 9.87 (1 H, s), 8.44 (1 H, d, *J*=2.02 Hz), 7.68 - 7.82 (2 H, m), 7.45 - 7.66 (4 H, m), 7.21 - 7.32 (2 H, m), 7.15 (1 H, d, *J*=8.34 Hz), 6.95 (1 H, d, *J*=15.41 Hz), 5.81 (1 H, s), 4.26 - 4.38 (1 H, m), 4.10 (2 H, d, *J*=6.06 Hz), 3.87 - 3.98 (1 H, m), 3.53 (3 H, s), 3.17 (1 H, d, *J*=18.95 Hz), 2.93 (1 H, br. s.), 2.67 (1 H, d, *J*=1.77 Hz). LCMS (ESI) *m/z*: 572.0 [M+H].⁺ HPLC purity > 95%. HPLC: *t_R* = 8.22 min.

(*S,E*)-2-(3-(5-chloro-2-(1*H*-tetrazol-1-yl)phenyl)acryloyl)-N-(1*H*-indazol-6-yl)-1,2,3,4-tetrahydroisoquinoline-1-carboxamide (19**).** Compound **19** was prepared in a similar manner as **6** using 1*H*-indazol-6-amine. ¹H NMR (400 MHz, CD₃OD) δ 9.53 (1 H, s), 8.17 (1 H, d, *J*=2.27 Hz), 8.01 (1 H, d, *J*=2.27 Hz), 7.62 - 7.73 (2 H, m), 7.56 (2 H, d, *J*=8.59 Hz), 7.36 (1 H, d, *J*=15.4 Hz), 7.26 - 7.31 (4 H, m), 7.21 (1 H, d, *J*=15.4 Hz), 7.13 (1 H, dd, *J*=8.72, 1.64 Hz), 5.89 (1 H, s), 4.29 - 4.36 (1 H, m), 3.87 (1 H, ddd, *J*=12.44, 8.65, 4.17 Hz), 3.29 - 3.35 (1 H, m),

2.92 - 3.02 (1 H, m). LCMS (ESI) m/z: 525.4 [M+H]⁺ HPLC purity > 95%. HPLC: t_R = 7.78 min.

(*S,E*)-*N*-(3-Amino-1*H*-indazol-6-yl)-2-(3-(5-chloro-2-(1*H*-tetrazol-1-yl)phenyl)acryloyl)-

1,2,3,4-tetrahydroisoquinoline-1-carboxamide (20). *Step 1.* 4-Amino-2-fluorobenzonitrile

(0.10 g, 0.75 mmol) was combined with (*S*)-2-(((9*H*-fluoren-9-yl)methoxy)carbonyl)-1,2,3,4-

tetrahydroisoquinoline-1-carboxylic acid (0.30 g, 0.75 mmol) in DCM (5 mL), and the mixture

was cooled in a water ice/acetone bath. Pyridine (0.30 mL, 3.8 mmol) was added, and then

POCl₃ (0.070 mL, 0.75 mmol) was carefully added dropwise. After 45 min, the reaction was

partitioned with 1 N HCl (15 mL) and EtOAc (40 mL). The organic layer was washed with

aqueous 0.1N HCl (10 mL) and brine (10 mL), dried (over MgSO₄), filtered and concentrated.

The resulting crude material was purified by silica gel column chromatography to afford (*S*)-

(9*H*-fluoren-9-yl)methyl 1-(4-cyano-3-fluorophenylcarbamoyl)-3,4-dihydroisoquinoline-2(1*H*)-

carboxylate (0.38 g, 98%) as a white foam. ¹H NMR (400 MHz, CDCl₃) δ 9.34 (1 H, br. s.), 7.77

(2 H, br. s.), 7.57 (3 H, d, *J*=7.58 Hz), 7.36 - 7.48 (3 H, m), 7.13 - 7.35 (7 H, m), 5.69 (1 H, br.

s.), 4.60 (2 H, d, *J*=7.07 Hz), 4.31 (1 H, br. s.), 3.74 (2 H, br. s.), 3.03 (1 H, br. s.), 2.88 (1 H, br.

s.). LCMS (ESI) m/z: 518.1 [M+H]⁺.

Step 2. To (*S*)-(9*H*-fluoren-9-yl)methyl 1-(4-cyano-3-fluorophenylcarbamoyl)-3,4-

dihydroisoquinoline-2(1*H*)-carboxylate (0.13 g, 0.25 mmol) in EtOH (10 mL) was added

hydrazine hydrate (0.060 mL, 2.0 mmol), and the reaction was heated at 160 °C for 11 min. in a

microwave apparatus. The solvents were removed, and the resulting crude (*S*)-*N*-(3-amino-1*H*-

indazol-6-yl)-1,2,3,4-tetrahydroisoquinoline-1-carboxamide was used in next step. LCMS (ESI)

m/z: 308.3 [M+H]⁺.

Step 3. Compound **20** (24 mg, 14%) was prepared in a similar manner described for **6** using (S)-N-(3-amino-1*H*-indazol-6-yl)-1,2,3,4-tetrahydroisoquinoline-1-carboxamide. ¹H NMR (400 MHz, CD₃OD) δ 9.53 (1 H, s), 8.19 (1 H, d, *J*=2.27 Hz), 7.94 (1 H, s), 7.84 (1 H, d, *J*=9.09 Hz), 7.67 (1 H, d, *J*=2.27 Hz), 7.55 - 7.62 (1 H, m), 7.52 (1 H, d, *J*=5.56 Hz), 7.38 (1 H, d, *J*=15.41 Hz), 7.25 - 7.33 (3 H, m), 7.12 - 7.24 (2 H, m), 5.82 (1 H, s), 4.33 (1 H, ddd, *J*=12.13, 5.31, 5.05 Hz), 3.73 - 3.89 (1 H, m), 3.32 - 3.41 (1 H, m), 2.97 (1 H, dt, *J*=15.60, 4.58 Hz). LCMS (ESI) *m/z*: 540.0 [M+H].⁺ HPLC purity > 95%. HPLC: *t_R* = 5.81 min.

(*S,E*)-Methyl 4-(2-(3-(3-chloro-2-fluoro-6-(1*H*-tetrazol-1-yl)phenyl)acryloyl)-1,2,3,4-tetrahydroisoquinoline-1-carboxamido)phenylcarbamate (**21**). Compound **21** (11 mg, 39%) was prepared in a similar manner as **17**. ¹H NMR (400 MHz, DMSO-*d*₆) δ 10.35 - 10.41 (1 H, m), 9.87 (1 H, s), 9.53 - 9.58 (1 H, m), 7.90 - 8.00 (1 H, m), 7.64 - 7.70 (1 H, m), 7.57 - 7.62 (1 H, m), 7.41 - 7.50 (2 H, m), 7.32 - 7.38 (2 H, m), 7.25 (4 H, d, *J*=3.03 Hz), 7.03 - 7.15 (1 H, m), 6.91 - 6.99 (1 H, m), 5.77 - 5.82 (1 H, m), 4.08 - 4.17 (1 H, m), 3.67 - 3.73 (1 H, m), 3.64 (3 H, s), 3.11 - 3.19 (1 H, m), 2.83 - 2.90 (1 H, m). LCMS (ESI) *m/z*: 576 [M+H].⁺ HPLC purity > 95%. HPLC: *t_R* = 8.7 min.

(*S,E*)-4-(2-(3-(3-chloro-2-fluoro-6-(1*H*-tetrazol-1-yl)phenyl)acryloyl)-1,2,3,4-tetrahydroisoquinoline-1-carboxamido)benzoic acid (**22**). Compound **22** (10 mg, 33%) was prepared in a similar manner as **6**. ¹H NMR (400 MHz, CD₃OD) δ 9.56 (1 H, s), 7.97 (2 H, d, *J*=8.84 Hz), 7.78 - 7.85 (1 H, m), 7.64 - 7.70 (2 H, m), 7.47 - 7.56 (2 H, m), 7.29 (4 H, d, *J*=2.53 Hz), 7.04 - 7.19 (2 H, m), 5.84 (1 H, s), 4.18 (1 H, ddd, *J*=12.00, 5.31, 5.18 Hz), 3.64 - 3.74 (1 H, m), 2.95 (1 H, dt, *J*=15.35, 4.83 Hz). LCMS (ESI) *m/z*: 547.3 [M+H].⁺ HPLC purity > 95%. HPLC: *t_R* = 6.76 min.

(E)-4-(2-(3-(5-chloro-2-(1H-tetrazol-1-yl)phenyl)acryloyl)-5-(methoxycarbonyl)-1,2,3,4-tetrahydroisoquinoline-1-carboxamido)benzoic acid (23). Compound **23** (4.4 mg, 15 %) was prepared from methyl 1,2,3,4-tetrahydroisoquinoline-5-carboxylate in a similar manner as described for **7**. ¹H NMR (400 MHz, CD₃OD) δ 9.54 (1 H, s), 8.21 (1 H, d, *J*=2.27 Hz), 7.96 (2 H, d, *J*=8.59 Hz), 7.89 (1 H, d, *J*=7.83 Hz), 7.68 - 7.77 (1 H, m), 7.60 - 7.68 (3 H, m), 7.55 - 7.60 (1 H, m), 7.33 - 7.45 (2 H, m), 7.17 - 7.29 (1 H, d, *J*=15.4 Hz), 5.91 (1 H, s), 4.31 (1 H, ddd, *J*=12.38, 5.43, 5.18 Hz), 3.93 (3 H, s), 3.81 (1 H, ddd, *J*=12.63, 8.97, 4.17 Hz), 3.56 - 3.68 (1 H, m), 3.44 - 3.57 (1 H, m). LCMS (ESI) *m/z*: 586.9[M+H].⁺ HPLC purity > 95%. HPLC: *t_R* = 8.52 min.

(E)-4-(2-(3-(5-Chloro-2-(1H-tetrazol-1-yl)phenyl)acryloyl)-5-(piperazin-1-yl)-1,2,3,4-tetrahydroisoquinoline-1-carboxamido)benzoic acid (43). *Step 1.* To 5-(piperazin-1-yl)isoquinoline hydrochloride (1.4 g, 5.6 mmol) in dioxane (6 mL), was added NaOH (12 mL, 12 mmol), and the solution was cooled in ice bath. To this solution was added Boc₂O (1.3 mL, 5.6 mmol), and the reaction was gradually warmed to rt overnight. After 24 h, the reaction was concentrated, and the residue was partitioned with water (30 mL) and EtOAc (100 mL). The organic layer was washed with brine (15 mL), dried (MgSO₄), filtered and concentrated to afford **73** (1.8 g, quant.) as a yellow oil. LCMS(ESI) *m/z*: 314.1 [M+H].⁺ The crude product was taken up in EtOH (40 mL), PtO₂ was added, and the mixture placed under a H₂ atmosphere at 55 psi for 48 h. Filtration through Celite[®] and concentration afforded *tert*-butyl 4-(1,2,3,4-tetrahydroisoquinolin-5-yl)piperazine-1-carboxylate (1.7 g, 94%) as an off-white foam. ¹H NMR (400 MHz, DMSO-*d*₆) δ 9.40 (1 H, br. s.), 7.20 - 7.34 (1 H, m), 7.02 - 7.13 (1 H, m), 6.91 - 7.01 (1 H, m), 4.24 (2 H, s), 3.48 (2 H, br. s.), 3.28 - 3.35 (4 H, m), 2.96 (2 H, t, *J*=5.94 Hz), 2.77 (4 H, t, *J*=4.80 Hz), 1.43 (9 H, s). LCMS (ESI) *m/z*: 318.1 [M+H].⁺

Step 2. *tert*-Butyl 4-(3,4-dihydroisoquinolin-5-yl)piperazine-1-carboxylate (**77**) (0.77 g, 98%), a dark foam, was prepared from *tert*-butyl 4-(1,2,3,4-tetrahydroisoquinolin-5-yl)piperazine-1-carboxylate by MnO₂ oxidation as described for **7**. ¹H NMR (400 MHz, CDCl₃) δ 8.34 (s, 1H), 7.42 - 7.21 (m, 1H), 7.10 (dd, *J*=8.1, 1.0 Hz, 1H), 7.03 (d, *J*=7.6 Hz, 1H), 3.83 - 3.66 (m, 2H), 3.58 (br s, 4H), 2.84 (br t, *J*=4.9 Hz, 4H), 2.75 - 2.47 (m, 2H), 1.49 (s, 9H). LCMS (ESI) *m/z*: 316.2 [M+H].⁺

Step 3. Compound **43** (18 mg, 7.5%) was prepared from **77** via the multicomponent Ugi coupling reaction as described for **7**. ¹H NMR (400 MHz, DMSO-*d*₆) δ 12.64 (1 H, br. s.), 10.68 (1 H, s), 9.79 (1 H, s), 8.60 (2 H, br. s.), 8.32 (1 H, d, *J*=2.02 Hz), 7.75 - 7.89 (2 H, m), 7.63 - 7.71 (2 H, m), 7.60 (1 H, d, *J*=8.84 Hz), 7.43 (1 H, d, *J*=15.41 Hz), 7.32 (1 H, d, *J*=7.58 Hz), 7.20 (1 H, t, *J*=7.83 Hz), 6.97 (1 H, d, *J*=8.08 Hz), 6.91 (1 H, d, *J*=15.41 Hz), 5.72 (1 H, s), 4.23 (1 H, d, *J*=5.56 Hz), 3.60 - 3.70 (1 H, m), 3.21 (4 H, br. s.), 2.85 - 3.11 (6 H, m). LCMS (ESI) *m/z*: 613.1 [M+H].⁺ HPLC purity > 95%. HPLC: *t*_R = 5.54 min.

(*E*)-4-(2-(3-(5-Chloro-2-(1*H*-tetrazol-1-yl)phenyl)acryloyl)-5-(4-(methoxycarbonyl)piperazin-1-yl)-1,2,3,4-tetrahydroisoquinoline-1-carboxamido)benzoic acid (44**)**. To **43** (6.9 mg, 9.5 μmol) in DCM (1 mL) was added DIEA (4.9 μL, 0.03 mmol) and methyl chloroformate (2.2 μL, 0.030 mmol). After 2 h, the reaction was concentrated, and the residue was dissolved in THF/water (2:1, 3 mL), and 1 M LiOH (0.5 mL) was added. The reaction was stirred for 15 min, acidified with TFA, and concentrated. The crude material was purified by reverse phase HPLC, and the collected purified fraction were lyophilized to afford **44** (3.8 mg, 45%) as a white solid. ¹H NMR (400 MHz, CD₃OD) δ 9.54 (1 H, s), 8.19 (1 H, d, *J*=2.27 Hz), 7.96 (2 H, d, *J*=8.59 Hz), 7.61 - 7.71 (3 H, m), 7.57 - 7.60 (1 H, m), 7.25 - 7.36 (3 H, m), 7.16 - 7.23 (1 H, d, *J*=15.4 Hz), 7.07 (1 H, dd, *J*=7.20, 1.64 Hz), 5.78 (1 H, s), 4.33 (1 H,

ddd, $J=12.00, 4.80, 4.67$ Hz), 3.74 (3 H, s), 3.59 - 3.72 (5 H, m), 3.22 (2 H, t, $J=5.68$ Hz), 2.94 - 3.01 (2 H, m), 2.89 (2 H, br. s.). LCMS (ESI) m/z : 671.1 $[M+H]^+$ HPLC purity > 95%. HPLC: $t_R = 8.49$ min.

(*E*)-4-(2-(3-(5-Chloro-2-(1*H*-tetrazol-1-yl)phenyl)acryloyl)-5-(2-oxopiperidin-1-yl)-1,2,3,4-tetrahydroisoquinoline-1-carboxamido)benzoic acid (45). *Step 1.* 1-(1,2,3,4-

Tetrahydroisoquinolin-5-yl)piperidin-2-one (0.38 g, 1.6 mmol) was oxidized with MnO_2 as described previously for **7** to afford 1-(3,4-dihydroisoquinolin-5-yl)piperidin-2-one (0.36 g, 98%) as a dark oil. 1H NMR (400 MHz, $CDCl_3$) δ 8.30 - 8.40 (1 H, m), 7.30 - 7.41 (1 H, m), 7.20 - 7.30 (2 H, m), 3.77 - 3.91 (1 H, m), 3.57 - 3.75 (2 H, m), 3.36 - 3.50 (1 H, m), 2.37 - 2.74 (4 H, m), 1.85 - 2.08 (4 H, m). LCMS (ESI) m/z : 229.0 $[M+H]^+$.

Step 2. Compound **45** (13 mg, 12%) was prepared using 1-(3,4-dihydroisoquinolin-5-yl)piperidin-2-one via the multicomponent Ugi coupling reaction as described for **7**. 1H NMR (400 MHz, CD_3OD) δ 9.54 (1 H, s), 8.17 (1 H, t, $J=2.78$ Hz), 7.90 - 8.03 (2 H, m), 7.61 - 7.73 (3 H, m), 7.56 - 7.60 (1 H, m), 7.52 (1 H, d, $J=7.83$ Hz), 7.29 - 7.44 (2 H, m), 7.14 - 7.27 (2 H, m), 5.87 - 5.94 (1 H, m), 4.19 - 4.32 (1 H, m), 3.82 - 3.98 (1 H, m), 3.63 - 3.73 (1 H, m), 3.45 - 3.54 (1 H, m), 2.98 - 3.11 (1 H, m), 2.76 - 2.89 (1 H, m), 2.50 - 2.62 (2 H, m), 2.02 (4 H, br. s.). LCMS (ESI) m/z : 626.0 $[M+H]^+$ HPLC purity > 95%. HPLC: $t_R = 7.46$ min.

(*S,E*)-4-(2-(3-(3-Chloro-2-fluoro-6-(1*H*-tetrazol-1-yl)phenyl)acryloyl)-5-morpholino-1,2,3,4-tetrahydroisoquinoline-1-carboxamido)benzoic acid (46). *Step 1.* A mixture of compound **69** (1.9 g, 9.4 mol), morpholine (0.82 mL, 9.4 mmol), and NaOtBu (1.3 g, 13 mmol) in toluene (10 mL) was degassed with Ar. To the reaction mixture was added BINAP (0.18 g, 0.28 mmol) and $Pd_2(dba)_3$ (86 mg, 0.09 mmol). The reaction mixture was heated to 130 °C in a microwave for 20 min. The reaction mixture was diluted with water (50 mL) and washed with (3 x 75 mL) of ethyl

acetate. The combined organic layer was washed with brine (50 mL), dried (MgSO₄), filtered and concentrated. The crude product was oxidized with MnO₂ as previously described for **7**.

Purification by silica gel chromatography afforded 4-(3,4-dihydroisoquinolin-5-yl)morpholine (2 g, 100%). ¹H NMR (400 MHz, CDCl₃) δ 9.23 (s, 1H), 8.53 (d, *J*=6.1 Hz, 1H), 7.93 (d, *J*=6.1 Hz, 1H), 7.68 (d, *J*=8.3 Hz, 1H), 7.58 - 7.36 (m, 1H), 7.31 - 7.12 (m, 1H), 4.19 - 3.86 (m, 4H), 3.24 - 2.89 (m, 4H). LCMS (ESI) *m/z*: 215.1 [M+H].⁺

Step 2. *tert*-Butyl (*S,E*)-4-(2-(3-(3-chloro-2-fluoro-6-(1*H*-tetrazol-1-yl)phenyl)acryloyl)-5-morpholino-1,2,3,4-tetrahydroisoquinoline-1-carboxamido)benzoate (1.2 g, 60%) was prepared by using 4-(3,4-dihydroisoquinolin-5-yl)morpholine and **58c** in the multicomponent Ugi coupling reaction as described for **7**. ¹H NMR (400 MHz, CD₃OD) δ 9.56 (1 H, s), 7.88 (2 H, d, *J*=8.59 Hz), 7.79 (1 H, d, *J*=7.83 Hz), 7.55 - 7.67 (2 H, m), 7.41 - 7.53 (1 H, m), 7.22 - 7.36 (2 H, m), 6.94 - 7.17 (3 H, m), 5.75 (1 H, s), 4.09 - 4.21 (1 H, m), 3.79 - 3.95 (4 H, m), 3.42 - 3.55 (1 H, m), 3.11 - 3.23 (2 H, m), 2.94 - 3.08 (2 H, m), 2.74 - 2.93 (2 H, m), 1.59 (9 H, s). LCMS (ESI) *m/z*: 688.3 [M+H].⁺ Chiral SFC separation of a sample (0.28 g) of the racemic mixture using Chiralpak AD-H, 250 X 21 mm, 5μm, using 55/45 CO₂/1:1 EtOH-IPA-0.1% DEA at 60 mL/min, 100 bar BP, 35 °C to afforded the desired enantiomer (89 mg, 95% ee) as white solid.

Step 3. To *tert*-butyl (*S,E*)-4-(2-(3-(3-chloro-2-fluoro-6-(1*H*-tetrazol-1-yl)phenyl)acryloyl)-5-morpholino-1,2,3,4-tetrahydroisoquinoline-1-carboxamido)benzoate (89 mg, 0.13 mmol) was added 30% TFA/DCM (6 mL). After 3 h, the reaction mixture was concentrated, and the residue was purified by reverse phase HPLC. and the product lyophilized to afford **46** (83 mg, 86%) as a white solid. ¹H NMR (400 MHz, CD₃OD) δ 9.44 (1 H, s), 7.84 (2 H, d, *J*=8.84 Hz), 7.69 (1 H, t, *J*=8.08 Hz), 7.53 (2 H, d, *J*=8.84 Hz), 7.38 (1 H, dd, *J*=8.72, 1.64 Hz), 7.10 - 7.26 (2 H, m), 6.89 - 7.07 (3 H, m), 5.64 (1 H, s), 3.98 - 4.09 (1 H, m), 3.69 - 3.89 (4 H, m), 3.33 - 3.46 (1 H, m),

3.00 - 3.10 (2 H, m), 2.85 - 2.94 (2 H, m), 2.76 (2 H, d, $J=3.54$ Hz). LCMS (ESI) m/z : 632.3

[$M+H$].⁺ HPLC purity > 95%. HPLC: t_R = 8.44 min.

(*S,E*)-4-(2-(3-(3-Chloro-2-fluoro-6-(1*H*-tetrazol-1-yl)phenyl)acryloyl)-5-thiomorpholino-1,2,3,4-tetrahydroisoquinoline-1-carboxamido)benzoic acid, TFA (47**)** *Step 1*. Compound **67**

(1.8 g, 98%), a yellow solid, was prepared as described for **46** using **66** (1.7 g, 5.4 mmol) and thiomorpholine (0.84 g, 8.1 mmol). ¹H NMR (400 MHz, CDCl₃) δ 7.10 - 7.24 (1 H, m), 6.78 - 7.00 (2 H, m), 4.51 - 4.67 (2 H, m), 3.53 - 3.71 (2 H, m), 3.09 - 3.25 (4 H, m), 2.71 - 2.91 (6 H, m), 1.48 - 1.58 (9 H, m). LCMS (ESI) m/z : 335.2 [$M+H$].⁺

Step 2. To **67** (0.99 g, 2.9 mmol) was added 30% TFA/DCM (6 mL), and the reaction mixture was stirred at rt for 2 h. The reaction was quenched with 1 N NaOH (10 mL) and extracted with DCM (3 x 30 mL). The combined organic layers were washed with brine (15 mL), dried (MgSO₄), filtered and concentrated to afford 4-(1,2,3,4-tetrahydroisoquinolin-5-yl)thiomorpholine (0.62g, 89%). ¹H NMR (400 MHz, CDCl₃) δ 7.27 - 7.22 (m, 1H), 7.03 (d, $J=7.8$ Hz, 1H), 6.87 (d, $J=7.8$ Hz, 1H), 4.32 (s, 2H), 3.41 (br t, $J=6.1$ Hz, 2H), 3.22 - 3.11 (m, 5H), 3.10 - 3.02 (m, 2H), 2.81 (br d, $J=3.0$ Hz, 4H). LCMS (ESI) m/z : 235.1 [$M+H$].⁺

Step 3. 4-(3,4-Dihydroisoquinolin-5-yl)thiomorpholine (77 mg, 53%), was prepared by oxidation of 4-(1,2,3,4-tetrahydroisoquinolin-5-yl)thiomorpholine with MnO₂ as described for **7**. ¹H NMR (400 MHz, CDCl₃) δ 8.34 (br s, 1H), 7.29 (br s, 2H), 7.14 (br s, 1H), 7.05 (br s, 1H), 3.73 (br s, 2H), 3.16 (br s, 5H), 2.82 (br s, 4H). LCMS (ESI) m/z : 233.1 [$M+H$].⁺

Step 4. Racemic **47** (65 mg, 24%) was prepared from 4-(3,4-dihydroisoquinolin-5-yl)thiomorpholine and **58c** via the multicomponent Ugi coupling reaction as described for **7**. The racemic product (65 mg) was purified via chiral SFC as previously described for **46** to afford **47** (14 mg, 19%, > 90% ee) as a white solid. ¹H NMR (400 MHz, CD₃OD) δ 9.53 (1 H, s), 7.94 (2

H, d, $J=8.84$ Hz), 7.79 (1 H, d, $J=7.83$ Hz), 7.59 - 7.73 (2 H, m), 7.48 (1 H, dd, $J=8.84$, 1.52 Hz), 7.20 - 7.36 (2 H, m), 6.97 - 7.19 (3 H, m), 5.75 (1 H, s), 4.06 - 4.21 (1 H, m), 3.43 - 3.59 (3 H, m), 3.00 - 3.25 (4 H, m), 2.73 - 2.96 (4 H, m). LCMS (ESI) m/z : 704.4 $[M+H]^+$. HPLC purity > 95%. HPLC: t_R = 10.61 min.

(*S,E*)-4-(2-(3-(3-Chloro-2-fluoro-6-(1*H*-tetrazol-1-yl)phenyl)acryloyl)-5-(1,1-dioxidothiomorpholino)-1,2,3,4-tetrahydroisoquinoline-1-carboxamido)benzoic acid (48).

Step 1. Compound **68** (0.45 g, 83 %), a tan solid, was obtained from thiomorpholine 1,1-dioxide (0.30 g, 2.2 mmol) as described for **47**. ^1H NMR (400 MHz, CDCl_3) δ 7.21 (1 H, t, $J=7.83$ Hz), 6.92 - 7.03 (2 H, m), 4.60 (2 H, s), 3.65 (2 H, t, $J=5.56$ Hz), 3.40 - 3.51 (4 H, m), 3.16 - 3.30 (4 H, m), 2.84 (2 H, t, $J=5.68$ Hz), 1.48 - 1.55 (9 H, m). LCMS (ESI) m/z : 367.2 $[M+H]^+$.

Step 2. Compound **48** (6 mg, 19%, 99.4% ee) was prepared in a similar manner as described for **47** substituting *tert*-butyl 5-(1,1-dioxidothiomorpholino)-3,4-dihydroisoquinoline-2(1*H*)-carboxylate for *tert*-butyl 5-thiomorpholino-3,4-dihydroisoquinoline-2(1*H*)-carboxylate and chirally purified via chiral SFC as described for **46**. ^1H NMR (400 MHz, CD_3OD) δ 9.44 (1 H, s), 7.84 (2 H, d, $J=8.59$ Hz), 7.65 - 7.76 (1 H, m), 7.53 (2 H, d, $J=8.84$ Hz), 7.38 (1 H, d, $J=8.59$ Hz), 7.14 - 7.28 (2 H, m), 6.99 - 7.11 (2 H, m), 6.88 - 6.98 (1 H, m), 5.69 (1 H, s), 3.98 - 4.11 (1 H, m), 3.41 - 3.55 (2 H, m), 3.28 - 3.42 (7 H, m), 3.00 - 3.17 (2 H, m). LCMS (ESI) m/z : 680.4 $[M+H]^+$. HPLC purity > 95%. HPLC: t_R = 7.80 min.

(*S,E*)-4-(2-(3-(3-Chloro-2-fluoro-6-(1*H*-tetrazol-1-yl)phenyl)acryloyl)-5-(piperidin-1-yl)-1,2,3,4-tetrahydroisoquinoline-1-carboxamido)benzoic acid (49). Compound **49** (38 mg, 20%) was prepared via the multicomponent Ugi coupling reaction as described for **47** substituting piperidine for morpholine. ^1H NMR (400 MHz, CD_3OD) δ 9.44 (1 H, s), 7.84 (2 H, d, $J=8.59$ Hz), 7.64 - 7.72 (1 H, m), 7.52 (2 H, dd, $J=8.72$, 1.39 Hz), 7.38 (2 H, dd, $J=8.84$, 1.52

Hz), 7.27 (2 H, d, $J=7.07$ Hz), 6.99 - 7.11 (1 H, m), 6.80 - 6.94 (1 H, m), 5.72 (1 H, s), 4.72 - 4.80 (2 H, m), 4.03 - 4.17 (1 H, m), 3.44 (1 H, t, $J=11.12$ Hz), 3.05 - 3.30 (5 H, m), 1.76 - 1.93 (3 H, m), 1.61 (2 H, br. s.). LCMS (ESI) m/z : 630.3 $[M+H]^+$. HPLC purity > 95%. HPLC: t_R = 7.46 min.

(*S,E*)-4-(2-(3-(3-Chloro-2-fluoro-6-(1*H*-tetrazol-1-yl)phenyl)acryloyl)-5-(4-(dimethylamino)piperidin-1-yl)-1,2,3,4-tetrahydroisoquinoline-1-carboxamido)benzoic acid

(50). *Step 1.* Compound **71** (1.2 g, 89 %) was prepared from *N,N*-dimethylpiperidin-4-amine (0.74 g, 5.8 mmol), as previously described for compound **47**. ^1H NMR (400 MHz, CDCl_3) δ 9.23 (d, $J=0.8$ Hz, 1H), 8.54 (d, $J=5.8$ Hz, 1H), 7.91 (d, $J=6.1$ Hz, 1H), 7.65 (d, $J=8.1$ Hz, 1H), 7.52 (t, $J=7.8$ Hz, 1H), 7.31 - 7.11 (m, 1H), 3.58 - 3.34 (m, 2H), 2.80 (td, $J=11.9, 2.0$ Hz, 2H), 2.47 - 2.30 (m, 7H), 2.18 - 2.00 (m, 2H), 1.93 - 1.77 (m, 2H). LCMS (ESI) m/z : 282.1 $[M+H]^+$.

Step 2. Compound **71** (1.2 g, 4.3 mmol) was reduced as described in **41** to afford (1.1 g, 100 %) of *N,N*-dimethyl-1-(1,2,3,4-tetrahydroisoquinolin-5-yl)piperidin-4-amine as a dark oil. ^1H NMR (400 MHz, CDCl_3) δ 7.11 - 6.94 (m, 1H), 6.81 (d, $J=7.6$ Hz, 1H), 6.67 (d, $J=7.6$ Hz, 1H), 3.97 (s, 2H), 3.17 - 2.98 (m, 4H), 2.69 (t, $J=5.7$ Hz, 2H), 2.60 - 2.49 (m, 2H), 2.27 (s, 6H), 1.94 - 1.79 (m, 3H), 1.75 (br s, 1H), 1.63 - 1.48 (m, 2H). LCMS (ESI) m/z : 260.2 $[M+H]^+$.

Step 3. 1-(3,4-Dihydroisoquinolin-5-yl)-*N,N*-dimethylpiperidin-4-amine (1.2 g, 95%), a dark oil, was prepared by MnO_2 oxidation as described for **7**. ^1H NMR (400 MHz, CDCl_3) δ 8.35 (t, $J=2.0$ Hz, 1H), 7.20 - 7.11 (m, 1H), 7.02 (d, $J=7.1$ Hz, 1H), 6.90 (br t, $J=8.8$ Hz, 1H), 3.92 - 3.69 (m, 1H), 3.24 - 3.06 (m, 2H), 2.98 - 2.84 (m, 1H), 2.76 - 2.62 (m, 4H), 2.54 - 2.34 (m, 7H), 2.09 - 1.95 (m, 2H), 1.78 - 1.63 (m, 2H). LCMS (ESI) m/z : 258.2 $[M+H]^+$.

Step 4. Compound **50** (26.5 mg, 37.1 %, 99 % ee) was prepared as previously described for compound **47** and purified via chiral SFC as previously described for compound **46**. ^1H NMR

(400 MHz, CD₃OD) δ 9.57 (1 H, s), 7.96 (2 H, d, J =8.59 Hz), 7.81 (1 H, t, J =8.08 Hz), 7.65 (2 H, d, J =8.59 Hz), 7.50 (1 H, dd, J =8.59, 1.26 Hz), 7.28 (2 H, q, J =7.75 Hz), 7.17 (1 H, d, J =15.92 Hz), 7.09 (1 H, dd, J =7.33, 1.52 Hz), 6.96 (1 H, d, J =15.92 Hz), 5.77 (1 H, s), 4.12 (1 H, d, J =11.87 Hz), 3.48 (1 H, ddd, J =11.75, 9.22, 4.55 Hz), 3.29 - 3.39 (3 H, m), 3.11 - 3.24 (2 H, m), 2.97 (6 H, s), 2.89 - 2.96 (1 H, m), 2.61 - 2.75 (1 H, m), 2.13 - 2.28 (2 H, m), 1.90 - 2.07 (2 H, m). LCMS (ESI) m/z : 673.5 [M+H].⁺ HPLC purity > 95%. HPLC: t_R = 5.37 min.

(*S,E*)-4-(2-(3-(3-Chloro-2-fluoro-6-(1*H*-tetrazol-1-yl)phenyl)acryloyl)-5-(2-methyl-1-oxo-2,8-diazaspiro[4.5]decan-8-yl)-1,2,3,4-tetrahydroisoquinoline-1-carboxamido)benzoic acid

(51). *Step 1.* Compound **70** (0.87 g, 78 %) was prepared as described for **71**. ¹H NMR (400 MHz, CDCl₃) δ 9.17 (s, 1H), 8.49 (d, J =6.1 Hz, 1H), 7.91 (d, J =5.8 Hz, 1H), 7.59 (d, J =8.1 Hz, 1H), 7.46 (t, J =7.8 Hz, 1H), 7.20 (dd, J =7.5, 0.9 Hz, 1H), 3.48 - 3.27 (m, 4H), 2.96 - 2.78 (m, 4H), 2.40 - 2.19 (m, 2H), 2.07 - 1.89 (m, 2H), 1.57 (br d, J =13.1 Hz, 2H). LCMS (ESI) m/z : 296.5 [M+H].⁺

Step 2. Compound **51** (50 mg, 68 %, 99.2 % ee) was prepared from **70** via the multicomponent Ugi coupling reaction and purified via chiral SFC as previously described for compound **46**. ¹H NMR (400 MHz, CD₃OD) δ 9.55 (1 H, s), 7.94 (2 H, d, J =8.59 Hz), 7.79 (1 H, t, J =8.08 Hz), 7.63 (2 H, d, J =8.59 Hz), 7.43 - 7.54 (2 H, m), 7.30 - 7.43 (2 H, m), 7.12 - 7.22 (1 H, d, J =15.9 Hz), 7.01 - 7.12 (1 H, d, J =15.9 Hz), 5.83 (1 H, s), 4.11 - 4.27 (1 H, m), 3.53 - 3.60 (1 H, m), 3.46 (3 H, t, J =6.95 Hz), 3.29 - 3.39 (2 H, m), 3.17 - 3.30 (2 H, m), 3.08 (1 H, br. s.), 2.90 (3 H, s), 2.01 - 2.38 (4 H, m), 1.67 - 1.89 (2 H, m). LCMS (ESI) m/z : 713.5 [M+H].⁺ HPLC purity > 95%. HPLC: t_R = 6.97 min.

(*S,E*)-4-(2-(3-(3-Chloro-2-fluoro-6-(1*H*-tetrazol-1-yl)phenyl)acryloyl)-5-(2-oxopiperidin-1-yl)-1,2,3,4-tetrahydroisoquinoline-1-carboxamido)benzoic acid (52). Compound **52** (32 mg,

46 %, >95 % ee) was prepared via the multicomponent Ugi coupling reaction as described for

46. ¹H NMR (400 MHz, CD₃OD) δ 9.53 (1 H, s), 7.89 - 8.02 (2 H, m), 7.78 (1 H, td, *J*=8.08, 3.03 Hz), 7.61 - 7.71 (2 H, m), 7.44 - 7.59 (2 H, m), 7.33 - 7.41 (1 H, m), 7.19 - 7.26 (1 H, m), 7.00 - 7.19 (2 H, m), 5.89 (1 H, d, *J*=2.53 Hz), 4.07 - 4.18 (1 H, m), 3.63 - 3.82 (2 H, m), 3.51 (1 H, m), 2.97 - 3.13 (1 H, m), 2.72 - 2.86 (1 H, m), 2.50 - 2.66 (2 H, m), 2.03 (4 H, m). LCMS (ESI) *m/z*: 644.1 [M+H]⁺ HPLC purity > 95%. HPLC: *t_R* = 7.62 min.

(*S,E*)-4-(2-(3-(3-Chloro-2-fluoro-6-(1*H*-tetrazol-1-yl)phenyl)acryloyl)-5-(3-oxomorpholino)-1,2,3,4-tetrahydroisoquinoline-1-carboxamido)benzoic acid (53**).** *Step 1.* To **69** (0.36 g, 1.7 mmol) and morpholin-3-one (0.18 g, 1.7 mmol) was added DMSO (4 mL), 1,10-phenanthroline (31 mg, 0.17 mmol) and K₂CO₃ (0.59 g, 4.3 mmol). The reaction mixture was degassed with N₂ for 0.5 h, then CuI (66 mg, 0.35 mmol) was added, and the reaction mixture was heated at 130 °C. After 24 h, the reaction was quenched with dilute NH₄OH (20 mL) and extracted with ethyl acetate (3 x 40 mL). The combined organic layers were washed with brine (15 mL), dried (MgSO₄), filtered and concentrated. Purification of the crude material by silica gel chromatography using DCM/MeOH as eluents afforded **72** (0.33 g, 82%) as a white solid. ¹H NMR (400 MHz, CDCl₃) δ 9.32 (1 H, s), 8.52 - 8.73 (1 H, m), 7.89 - 8.07 (2 H, m), 7.54 - 7.73 (2 H, m), 4.33 - 4.58 (2 H, m), 4.02 - 4.22 (2 H, m), 3.81 - 3.90 (1 H, m), 3.66 - 3.81 (1 H, m). LCMS (ESI) *m/z*: 229.1 [M+H]⁺

Step 2. Compound **72** was oxidized with MnO₂ as described for **7** to afford **75** (287 mg, 83 %).

¹H NMR (400 MHz, CDCl₃) δ 8.28 (s, 1H), 7.52 (d, *J*=8.0 Hz, 1H), 7.29 (dd, *J*=8.0, 7.9 Hz, 1H), 7.08 (d, *J*=7.9 Hz, 1H), 4.36-4.29 (m, 2H), 4.16 (ddd, *J*=4.5, 3.2, -13.2 Hz, 1H), 4.16 (ddd, *J*=12.2, 4.5, -13.2 Hz, 1H), 3.87 (dt, *J*=16.1, 7.5 Hz, 1H), 3.79 (ddd, *J*=4.5, 3.2, -12.1 Hz, 1H),

3.79 (dt, $J=16.1$, 7.5 Hz, 1H), 3.63 (ddd, $J=12.2$, 4.5, -12.1 Hz, 1H), 2.94 (dt, $J=16.0$, 7.5 Hz, 1H), 2.85 (dt, $J=16.0$, 7.5 Hz, 1H). LCMS (ESI) m/z : 231.1 $[M+H]^+$.

Step 3. The desired enantiomer *tert*-Butyl (*S,E*)-4-(2-(3-(3-chloro-2-fluoro-6-(1*H*-tetrazol-1-yl)phenyl)acryloyl)-5-(3-oxomorpholino)-1,2,3,4-tetrahydroisoquinoline-1-carboxamido)benzoate (227 mg, 30 %, >95 % ee) was prepared via the multicomponent Ugi coupling reaction and separated as the second eluting enantiomer via chiral SFC separation, as previously described for compound **46**. ^1H NMR (400 MHz, CD_3OD) δ 9.53 (1 H, s), 7.88 - 8.08 (2 H, m), 7.79 (1 H, d, $J=7.58$ Hz), 7.58 - 7.71 (2 H, m), 7.51 - 7.61 (1 H, m), 7.47 - 7.51 (1 H, m), 7.38 (1 H, d, $J=7.58$ Hz), 7.25 - 7.35 (1 H, m), 6.98 - 7.21 (2 H, m), 5.89 - 5.91 (1 H, m), 4.22 - 4.44 (2 H, m), 4.01 - 4.17 (2 H, m), 3.73 - 3.85 (1 H, m), 3.55 - 3.66 (1 H, m), 3.13 (2 H, dt, $J=3.28$, 1.64 Hz), 2.71 - 2.92 (2 H, m), 1.57 (s, 9H). LCMS (ESI) m/z : 702.1 $[M+H]^+$.

Step 4. Compound **53** (41 mg, 75 %) was prepared by deprotection of *tert*-Butyl (*S,E*)-4-(2-(3-(3-chloro-2-fluoro-6-(1*H*-tetrazol-1-yl)phenyl)acryloyl)-5-(3-oxomorpholino)-1,2,3,4-tetrahydroisoquinoline-1-carboxamido)benzoate from step 3 using TFA (1 mL) in DCM (2 mL). The crude product was purified via reverse phase HPLC and lyophilized to afford a white solid. ^1H NMR (400 MHz, CD_3OD) δ 9.53 (1 H, s), 7.88 - 8.08 (2 H, m), 7.79 (1 H, d, $J=7.58$ Hz), 7.58 - 7.71 (2 H, m), 7.51 - 7.61 (1 H, m), 7.47 - 7.51 (1 H, m), 7.38 (1 H, d, $J=7.58$ Hz), 7.25 - 7.35 (1 H, m), 6.98 - 7.21 (2 H, m), 5.89 - 5.91 (1 H, m), 4.22 - 4.44 (2 H, m), 4.01 - 4.17 (2 H, m), 3.73 - 3.85 (1 H, m), 3.55 - 3.66 (1 H, m), 3.13 (2 H, dt, $J=3.28$, 1.64 Hz), 2.71 - 2.92 (2 H, m). LCMS (ESI) m/z : 646.0 $[M+H]^+$. HPLC purity > 95%. HPLC: t_R = 7.15 min.

(*S,E*)-4-(2-(3-(3-Chloro-2-fluoro-6-(1*H*-tetrazol-1-yl)phenyl)acryloyl)-5-(2-oxopiperazin-1-yl)-1,2,3,4-tetrahydroisoquinoline-1-carboxamido)benzoic acid (54**).** *Step 1.* Compound **77** (0.97 g, 65 %) was prepared as described previously for **75**. ^1H NMR (400 MHz, CDCl_3) δ 8.39

(t, $J=2.1$ Hz, 1H), 7.54 - 7.37 (m, 1H), 7.30-7.26 (m, 2H), 3.82 - 3.70 (m, 3H), 3.66 (t, $J=5.3$ Hz, 2H), 3.58 - 3.47 (m, 1H), 3.41 (td, $J=5.3, 2.8$ Hz, 2H), 2.77 - 2.61 (m, 1H), 2.56 - 2.38 (m, 1H), 1.50 (s, 9H). LCMS (ESI) m/z : 330.1 $[M+H]^+$.

Step 2. Compound **54** (83 mg, 29 %, 97.2 % ee), a white solid, was prepared in a similar manner as **53**, and purified by chiral SFC as previously described for **46**. ^1H NMR (400 MHz, CD_3OD) δ 9.45 (1 H, s), 7.79 - 7.97 (2 H, m), 7.64 - 7.75 (1 H, m), 7.46 - 7.64 (3 H, m), 7.30 - 7.44 (2 H, m), 7.15 - 7.27 (1 H, m), 6.99 - 7.15 (1 H, m), 6.75 - 6.88 (1 H, m), 5.82 (1 H, d, $J=3.28$ Hz), 3.83 - 4.11 (4 H, m), 3.52 - 3.74 (4 H, m), 2.93 - 3.05 (1 H, m), 2.72 (1 H, br. s.). LCMS (ESI) m/z : 645.3-647.3 $[M+H]^+$. HPLC purity > 95%. HPLC: t_R = 4.87 min.

(*S,E*)-4-(2-(3-(3-Chloro-2-fluoro-6-(1*H*-tetrazol-1-yl)phenyl)acryloyl)-5-(4-methyl-2-oxopiperazin-1-yl)-1,2,3,4-tetrahydroisoquinoline-1-carboxamido)benzoic acid (55**).** *Step 1.*

4-Methylpiperazin-2-one (1.0 g, 9.0 mmol) was subjected to the Ullmann reaction described in the preparation for **53** to afford **74** (0.59 g, 31 %) as a pale yellow solid. ^1H NMR (400 MHz, CDCl_3) δ 9.34 (s, 1H), 8.59 (d, $J=5.8$ Hz, 1H), 8.01 (d, $J=7.8$ Hz, 1H), 7.73 - 7.67 (m, 1H), 7.66 - 7.61 (m, 1H), 7.57 (d, $J=6.1$ Hz, 1H), 3.87 - 3.75 (m, 1H), 3.73 - 3.63 (m, 1H), 3.43 (d, $J=1.8$ Hz, 2H), 2.98 - 2.87 (m, 2H), 2.50 (s, 3H). LCMS (ESI) m/z : 242.1 $[M+H]^+$.

Step 2. Compound **74** (0.4 g, 1.66 mmol) was reduced by catalytic hydrogenation as previously described to afford 4-methyl-1-(1,2,3,4-tetrahydroisoquinolin-5-yl)piperazin-2-one (0.4 g, quant). ^1H NMR (400 MHz, CDCl_3) δ 7.25 - 7.15 (m, 1H), 7.03 (d, $J=7.6$ Hz, 2H), 4.13 - 3.99 (m, 2H), 3.67 (ddd, $J=11.7, 7.1, 4.4$ Hz, 1H), 3.55 - 3.43 (m, 1H), 3.38 - 3.23 (m, 2H), 3.23 - 3.06 (m, 2H), 2.89 - 2.73 (m, 2H), 2.73 - 2.64 (m, 1H), 2.63 (s, 1H), 2.61 - 2.50 (m, 1H), 2.43 (s, 3H). LCMS (ESI) m/z : 246.1 $[M+H]^+$.

Step 3. Compound **76** was prepared by MnO₂ oxidation of 4-methyl-1-(1,2,3,4-tetrahydroisoquinolin-5-yl)piperazin-2-one, as previously described for **7**. ¹H NMR (400 MHz, CDCl₃) δ 8.29 (t, *J*=2.1 Hz, 1H), 7.39 - 7.25 (m, 1H), 7.24 - 7.16 (m, 2H), 3.83 - 3.73 (m, 1H), 3.67 - 3.54 (m, 2H), 3.50 - 3.37 (m, 1H), 3.22 (s, 2H), 2.80 - 2.67 (m, 2H), 2.64 - 2.53 (m, 1H), 2.50 - 2.40 (m, 1H), 2.35 (s, 3H). LCMS (ESI) *m/z*: 244.1 [M+H].⁺

Step 4. (*E*)-*tert*-Butyl 4-(2-(3-(3-chloro-2-fluoro-6-(1*H*-tetrazol-1-yl)phenyl)acryloyl)-5-(4-methyl-2-oxopiperazin-1-yl)-1,2,3,4-tetrahydroisoquinoline-1-carboxamido)benzoate (0.34 g, 33%) was prepared via the multicomponent Ugi coupling reaction using **76** as described for **7**. ¹H NMR (400 MHz, CD₃OD) δ 9.44 (1 H, s), 7.74 - 7.84 (2 H, m), 7.62 - 7.73 (1 H, m), 7.43 - 7.58 (3 H, m), 7.37 (1 H, dd, *J* = 8.72, 1.64 Hz), 7.31 (1 H, td, *J* = 7.83, 2.78 Hz), 7.19 (1 H, t, *J* = 6.82 Hz), 6.98 - 7.11 (1 H, m), 6.79 - 6.94 (1 H, m), 5.80 (1 H, s), 3.94 - 4.20 (3 H, m), 3.84 - 3.95 (1 H, m), 3.62 - 3.80 (3 H, m), 3.53 - 3.64 (1 H, m), 2.99 (3 H, s), 2.92 - 2.96 (1 H, m), 2.61 - 2.77 (1 H, m), 1.47 (9 H, d, *J* = 2.02 Hz). LCMS (ESI) *m/z*: 715.3 [M+H].⁺

Step 4. Compound **55** (104 mg, 27.7 %, 99.6 % ee) was prepared as described previously for compound **53**. The single chiral enantiomer was isolated as the second eluting peak using chiral SFC conditions, as described for **46**, followed by deprotection in 30% TFA/DCM (25 mL) for 2 h and purification by HPLC. ¹H NMR (500MHz, DMSO-d₆ δ ppm 10.76 - 10.23 (m, 1H), 9.73 (s, 1H), 7.87 (d, *J* = 8.5 Hz, 2H), 7.87 - 7.83 (m, 1H), 7.68 (d, *J* = 8.8 Hz, 2H), 7.68 - 7.62 (m, 1H), 7.58 (dd, *J* = 8.7, 1.0 Hz, 1H), 7.35 (t, *J* = 7.8 Hz, 1H), 7.24 (d, *J* = 7.2 Hz, 1H), 6.99 (br. s., 2H), 5.98 (br. s., 1H), 4.07 - 3.99 (m, 1H), 3.98 - 3.85 (m, 3H), 3.77 (br. s., 1H), 3.69 (br. s., 1H), 3.60 (t, *J* = 5.6 Hz, 1H), 2.87 (s, 3H), 3.10 - 2.59 (m, 2H). ¹³C NMR (126MHz, DMSO-d₆) δ 169.19, 166.65, 164.67, 161.38, 155.54 (d, *J*=253.2 Hz), 145.04, 142.58, 139.36, 133.39, 131.99, 131.00, 130.15, 128.40, 128.16 - 127.68, 127.39, 127.29- 126.93, 126.41, 126.00, 123.95, 123.29

(d, J=19.7 Hz), 122.17 (d, J=16.2 Hz), 119.09, 60.14 -56.97, 54.57, 49.40, 46.32, 42.02, 41.84 - 41.59, 23.97. ^{19}F NMR (471MHz, DMSO- d_6) δ 109.71, 112.35 (m, 1F). LCMS (ESI) m/z: 659.3 [M+H] $^{+}$. HPLC Purity = 99.3% based on HPLC/UV area % at 220 with retention time of 12.31 min (column: Xbridge Phenyl 150mm (L) x 4.6mm (ID), 3.5 μm). The ee for **55** was > 99.7% (Column: Chiralpak AD-H, 250 X 4.6 mm ID, 5 μm , mobile phase 55/45, CO $_2$ /ethanol/2-propanol -0.1 v/v% DEA). High resolution mass spectrum observed 659.19250, calcd. 659.19280

ENZYME AFFINITY ASSAYS

Factors IXa, Xa, XIa, and activated protein C (aPC) were purchased from Haematologic Technologies. Factor XIIa, plasmin and recombinant single chain tissue-type plasminogen activator (tPA) were purchased from American Diagnostica. α -Thrombin and plasma kallikrein were purchased from Enzyme Research Laboratories. Urokinase was purchased from Abbott Laboratories. Trypsin and chymotrypsin were purchased from Sigma Aldrich. Tissue kallikrein-1 was obtained from Dr. Julie Chao, Medical University of South Carolina. Recombinant factor VIIa was purchased from Novo Nordisk. Recombinant soluble tissue factor residues 1-219 was produced at Bristol Myers Squibb.

Final concentrations of enzymes in the assays are given in parentheses. Factor XIa (0.05 nM), factor XIIa (4 nM), plasma kallikrein (0.2 nM), chymotrypsin (2 nM), tPA (4.3 nM), plasmin (3 nM) and urokinase (3.9 nM) assays were conducted in 50 mM HEPES pH 7.4, 145 mM sodium chloride, 5 mM potassium chloride, and 0.1 % PEG 8000. Factor Xa (1 nM), thrombin (0.2 nM), tissue kallikrein-1 (0.05 nM), trypsin (0.42 nM), and aPC (1.25 nM) assays were conducted in 100 mM sodium phosphate pH 7.4, 200 mM sodium chloride, and 0.5 % PEG 8000. Factor VIIa (10 nM) assays were conducted in 50 mM HEPES pH 7.4, 150 mM sodium chloride, 5 mM calcium

chloride, and 0.1% PEG 8000 and soluble tissue factor (40 nM). Factor IXa (30 nM) assays were conducted in 50 mM TRIS pH 7.4, 100 mM sodium chloride, 5 mM calcium chloride, 0.5 % PEG 8000 and 2 % DMSO and 100 nM hirudin (Berlex Laboratories). Activated rabbit plasma kallikrein was generated following a procedure described for human plasma kallikrein [see J Lab Clin Med. 1987 May;109(5):601-7]. Plasma was acidified with an equal volume of 1/6 N HCl. After 15 minutes, 0.1 M sodium phosphate pH 7.6, 0.15 M NaCl, and 0.001 M EDTA buffer, and 1/6 N NaOH, each in an equal volume to the original plasma volume was added to neutralize the acidified plasma. This procedure is reported to inactivate the endogenous plasma inhibitors of plasma kallikrein. Plasma prekallikrein was activated by adding 1/10 volume Actin® FSL aPTT reagent (Siemens) to acidified-neutralized plasma in a siliconized glass tube incubated for 5 minutes at 37 °C. The peptide substrates were (final substrate concentrations shown in parentheses: pyro-Glu-Pro-Arg-pNA(para-nitroaniline), (Diapharma) for factor XIa (250 to 1,500 μM), thrombin (283 μM), and aPC (500 μM); N-benzoyl-Ile-Glu-(OH, OMe)-Gly-Arg-pNA (Diapharma) for factor Xa (350 μM) and trypsin (153 μM); Methylsulfonyl-D-cyclohexylglycyl-Gly-Arg-AMC(7-amino-4-methylcoumarin) (Pentapharm) for factor IXa (400 μM); H-(D)-Ile-Pro-Arg-pNA (Diapharma) for factor VIIa (1,000 μM); H-(D) -CHT-Gly-Arg-pNA (American Diagnostica) for factor XIIa (150 μM); H-D-Pro-Phe-Arg-pNA (Diapharma) for plasma kallikrein (300 μM); H-D-Val-Leu-Arg-AFC for tissue kallikrein-1 (90 μM); MeO-Suc-Arg-Pro-Tyr-pNA (Diapharma) for chymotrypsin (150 μM); H-(D)-Val-Leu-Lys-pNA (Diapharma) for plasmin (480 μM); Methylsulfonyl-D-cyclohexylalanyl-Gly-Arg-pNA (American Diagnostica) for tPA (300 μM); pyro-Glu Gly-Arg-pNA (Diapharma) for urokinase (75 μM).

All assays were conducted at 37 °C, except where noted, in 96-well microtiter plate spectrophotometers or spectrofluorometers (Molecular Devices) with simultaneous measurement

of enzyme activities in control and inhibitor containing solutions. Compounds were dissolved and diluted in DMSO and analyzed at a final concentration of 1 % DMSO except where noted. Assays were initiated by adding enzyme to buffered solutions containing substrate in the presence or absence of inhibitor. Hydrolysis of the substrate resulted in the release of pNA (para - nitroaniline), which was monitored spectrophotometrically by measuring the increase in absorbance at 405 nm, or the release of AMC(7-amino-4-methylcoumarin), which was monitored spectrofluorometrically by measuring the increase in emission at 460 nm with excitation at 380 nm, or the release of AFC(7-amino-4-trifluoromethylcoumarin), which was monitored spectrofluorometrically by measuring the increase in emission at 505 nm with excitation at 400 nm. The rate of absorbance or fluorescence change is proportional to enzyme activity. A decrease in the rate of absorbance or fluorescence change in the presence of inhibitor is indicative of enzyme inhibition. Assays were conducted under conditions of excess substrate (up to 4 times K_m) and inhibitor over enzyme. The Michaelis constant, K_m , for substrate hydrolysis by each protease was determined by fitting data from independent measurements at several substrate concentrations to the Michaelis-Menten equation: $v = (V_{max} * [S]) / (K_m + [S])$ where v is the observed velocity of the reaction; V_{max} is the maximal velocity; $[S]$ is the concentration of substrate; K_m is the Michaelis constant for the substrate.

IC_{50} values were determined by allowing the protease to react with the substrate in the presence of the inhibitor. Reactions were allowed to go for periods of 10 - 120 minutes (depending on the protease) and the velocities (rate of absorbance or fluorescence change versus time) were measured. The following relationships were used to calculate IC_{50} values: $v_s/v_o = A + ((B-A) / (1 + (IC_{50}/I)^n))$ and where v_o is the velocity of the control in the absence of inhibitor; v_s is the velocity in the presence of inhibitor; I is the concentration of inhibitor; A is the minimum activity

remaining (usually locked at zero); B is the maximum activity remaining (usually locked at 1.0); n is the Hill coefficient, a measure of the number and cooperativity of potential inhibitor binding sites; IC₅₀ is the concentration of inhibitor that produces 50% inhibition. When negligible enzyme inhibition was observed at the highest inhibitor concentration tested the value assigned as a lower limit for IC₅₀ is the value that would be obtained with either 25 % or 50 % inhibition at the highest inhibitor concentration. In all other cases IC₅₀ values represent the average of duplicate determinations obtained over 8 to 11 concentrations. The intraassay and interassay variabilities are 5 % and 20 %, respectively. Competitive inhibition was assumed for all proteases. IC₅₀ values were converted to K_i values by the relationship: $K_i = IC_{50} / (1 + [S]/K_m)$.

COAGULATION ASSAYS

Coagulation assays were performed in a temperature-controlled automated coagulation device (Sysmex CA - 6000 or CA - 1500, Dade-Behring) according to the reagent manufacturer's instructions. Blood was obtained from healthy volunteers by venipuncture and anticoagulated with one-tenth volume 0.11 M buffered sodium citrate (Vacutainer, Becton Dickinson). Plasma was obtained after centrifugation at 2,000 g for 10 minutes and kept on ice prior to use. An initial stock solution of the inhibitor at 10 mM was prepared in DMSO. Subsequent dilutions were done in plasma. Clotting time was determined on control plasma, and plasma containing up to 7 different concentrations of inhibitor. Determinations were performed in duplicate and expressed as a mean ratio of treated vs. baseline control. The concentrations required to produce a 50% increase in the clotting time relative to the clotting time in the absence of the inhibitor (EC_{1.5x}) were calculated by linear interpolation (Microsoft Excel, Redmond, WA, USA) and are expressed as total plasma concentrations, not final assay concentrations after addition of clotting assay reagents. The aPTT reagents (Alexin or Actin[®] FSL) were from commercial sources. The aPTT reagent Actin[®] FSL,

which was used after the aPTT reagent Alexin was discontinued by the vendor, was used for compounds 15, 17, 21, and 23.

IN VIVO EFFICACY

Rabbit AV-shunt thrombosis and cuticle bleeding models

For a full description of the models see Wong et al.^{11a,b} Male New Zealand White rabbits (2 – 4 kg) were obtained from Covance (Denver, PA). Experiments were conducted in accordance with the regulations of the Animal Care and Use Committee of the Bristol-Myers Squibb Company. Briefly, male New Zealand White rabbits were anesthetized with ketamine (50 mg/kg IM) and xylazine (10 mg/kg IM), and their femoral artery, jugular vein and femoral vein were catheterized. These anesthetics were supplemented as needed. Thrombosis was induced by an arteriovenous (AV)-shunt device containing a silk thread. Blood flowed from the femoral artery via the AV-shunt into the opposite femoral vein for 40 min. The shunt was then disconnected and the silk thread covered with thrombus was weighed.

After obtaining a control AV-shunt thrombus weight, **55** was given by a bolus injection supplemented with a continuous IV infusion 30 min prior to the placement of the AV-shunt thrombosis. The thrombosis was induced by the AV-shunt using the same method as described above. The IV infusion of **55** was continued throughout the experiment.

Doses of **55** studied were (mg/kg + mg/kg/h IV) 0.023 + 0.155 and 0.23 + 1.55. The vehicle was 10% N,N-dimethylacetamide:25% PEG300:65% of 5% dextrose. The bolus was 1 ml/kg and the infusion rate was 2 ml/kg/h.

The rabbit cuticle bleeding time model, described by Wong et al.^{11b}, was used in this study. Bleeding time was defined as the time after cuticle transection when bleeding ceased. **55** at 0.46

mg/kg+3.1 mg/kg/h IV, ASA at 4 mg/kg/h IV, the combination of ASA (4 mg/kg/h) and **55** (0.46 mg/kg+3.1 mg/kg/h) or vehicle (as described above) was administered IV as described above 30 to 60 min prior to cuticle transection. Bleeding time was measured before and after treatment in opposite hind-limbs, and was expressed as a ratio of treated over the control value.

ASSOCIATED CONTENT

The supporting information is available free of charge on the ACS Publication website at DOI:

Molecular formular strings (CSV)

Experimental data ¹HNMR, LCMS, HPLC purity, chiral separation techniques and methods used, including descriptions for key intermediates **58-61**, and for compounds **12-15**, **25-42**. Also included CADD experimental section and Factor XIa/crystal structures data collections and structure refinement, solubility and solution stability experiments and single crystal x-ray information for **55**.

ACCESSION CODES

Crystallographic structures of 4, 6, 21, and 38 complexed to Factor XIa have been deposited in the PDB IDs 5QCK, 5QCL, 5QCM, and 5QCN respectively. Authors will release the atomic coordinates and experimental data upon article publication.

ACKNOWLEDGEMENT

The authors wish to thank Dr. James Corte, Joanne Smallheer for proofreading this manuscript, to colleagues at Biocon Bristol-Myers Research Center (BBRC), Bangalore, India, Dauh-Rung Wu and Peng Li for SFC support and Richard Rampulla for providing valuable synthetic reagents, and to Dr. Hyunsoo Park for providing single crystal x-ray crystallographic information on **55**.

AUTHOR INFORMATION

Corresponding Author

*E-mail: donald.pinto@bms.com, Phone: 609-466-5068

ABBREVIATIONS USED

FXI, Factor XI; FXIa, Factor XIa; DVT, deep vein thrombosis; ACS, acute coronary syndrome; aPTT, activated partial thromboplastin time; PT, prothrombin time, $EC_{1.5x}$, effective concentration which produces a 50% increase in the clotting time relative to the clotting time in the absence of the inhibitor; HLM, human liver microsome, THIQ, tetrahydroisoquinoline.

REFERENCES

- (1) (a) Wang, H.; et al. Global, regional, and national life expectancy, all-cause mortality, and cause-specific mortality for 249 causes of death, 1980–2015: a systematic analysis for the Global Burden of Disease Study 2015. *Lancet* **2016**, 388, 1459-1544. (b) ISTH Steering Committee for World Thrombosis Day. Thrombosis: a major contributor to the global disease burden. *J Thromb Haemost.* **2014**, 12, 1580–90.
- (2) (a) Kearon, C.; Akl, E. A.; Ornelas, J.; Blaivas, A.; Jimenez, D.; Bounameaux, H.; Huisman, M.; King, C. S.; Morris, T. A.; Sood, N.; Stevens, S. M.; Vintch, J. R. E.; Wells, P.; Woller, S. C.; Moores, L. Antithrombotic Therapy for VTE Disease, *Chest* **2016**, 149, 315-352. (b) January, C.T.; Wann, L.S.; Alpert, J.S.; Calkins, H.; Cigarroa, J. E.; Cleveland, J. C., Jr; Conti, J. B.; Ellinor, P. T.; Ezekowitz, M. D.; Field, M. E.; Murray, K. T.; Sacco, R. L.; Stevenson, W. G.; Tchou, P. J.; Tracy, C. M.; Yancy, C. W.; ACC/AHA Task Force Members. 2014 AHA/ACC/HRS guideline for the management of patients with atrial fibrillation: a report of the American College

of Cardiology/American Heart Association Task Force on practice guidelines and the Heart Rhythm Society. *Circulation* **2014**, *130*, e199-e267. (c) Levine, G. N.; Bates, E. R.; Bittl, J. A.; Brindis, R. G.; Fihn, S. D.; Fleisher, L. A.; Granger, C. B.; Lange, R. A.; Mack, M. J.; Mauri, L.; Mehran, R.; Mukherjee, D.; Newby, L. K.; O’Gara, P. T.; Sabatine, M. S.; Smith, P. K.; Smith, S. C. 2016 ACC/AHA Guideline Focused Update on Duration of Dual Antiplatelet Therapy in Patients With Coronary Artery Disease: A Report of the American College of Cardiology/American Heart Association Task Force on Clinical Practice Guidelines: An Update of the 2011 ACCF/AHA/SCAI Guideline for Percutaneous Coronary Intervention, 2011 ACCF/AHA Guideline for Coronary Artery Bypass Graft Surgery, 2012 ACC/AHA/ACP/AATS/PCNA/SCAI/STS Guideline for the Diagnosis and Management of Patients With Stable Ischemic Heart Disease, 2013 ACCF/AHA Guideline for the Management of ST-Elevation Myocardial Infarction, 2014 AHA/ACC Guideline for the Management of Patients With Non–ST-Elevation Acute Coronary Syndromes, and 2014 ACC/AHA Guideline on Perioperative Cardiovascular Evaluation and Management of Patients Undergoing Noncardiac Surgery. *Circulation* **2016**, *134*, e123-e155. (d) Hirsh, J.; Fuster, V.; Ansell, J.; Halperin, J. L.; American Heart Association; American College of Cardiology Foundation. American Heart Association/American College of Cardiology Foundation guide to warfarin therapy. *Circulation* **2003**, *107*, 1692-711.

(3) Hirsh, J.; Anand, S. S.; Halperin, J. L.; Fuster, V.; American Heart Association. Guide to anticoagulant therapy: Heparin : a statement for healthcare professionals from the American Heart Association. *Circulation* **2001**, *103*, 2994-3018.

(4) (a) Gailani, D. and Gruber, A. Factor XI as a Therapeutic Target. *Arterioscler. Thromb. Vasc. Biol.* **2016**, *36*, 1316-1322. (b) Rosenthal, R.; Dreskin, O.; Rosenthal, N. New hemophilia-like

disease caused by deficiency of a third plasma thromboplastin factor. *Proc Soc Exp Biol Med.* **1953**, 82, 171-174. (c) Meijers, J. C.; Tekelenburg, W. L.; Bouma, B. N.; Bertina, R. M.; Rosendaal, F. R. High levels of coagulation factor XI as a risk factor for venous thrombosis. *N. Engl. J. Med.* **2000**, 342, 696-701. (d) Salomon, O.; Steinberg D. M.; Koren-Morag, N.; Tanne, D.; Seligsohn, U. Reduced incidence of ischemic stroke in patients with severe factor XI deficiency. *Blood* **2008**, 111, 4113-4117.

(5) (a) Schumacher, W. A., Seiler, S. E., Steinbacher, T. E., Stewart, A. B., Bostwick, J. S., Hartl, K. S., Liu, E. C., Ogletree, M. L.. Antithrombotic and hemostatic effects of a small molecule factor XIa inhibitor in rats. *Eur J Pharmacol.* **2007**, 570, 167-174. (b) Wong, P. C.; Crain, E. J., Watson, C. A.; Schumacher, W. A.; A small-molecule factor XIa inhibitor produces antithrombotic efficacy with minimal bleeding time prolongation in rabbits. *J Thromb Thrombolysis* **2011**, 32, 129-137. The β -lactam has been referred to in the literature as BMS-262084. (c) Rosen, E. D.; Gailani, D.; Castellino, F. J. FXI is essential for thrombus formation following FeCl₃-induced injury of the carotid artery in the mouse. *Thromb. Haemost.* **2002**, 87, 774-776. (d) Wang, X.; Cheng, Q.; Xu, L.; Feuerstein, G. Z.; Hsu, M. Y.; Smith, P. L.; Seiffert, D. A.; Schumacher, W. A.; Ogletree, M. L.; Gailani, D. Effects of factor IX or factor XI deficiency on ferric chloride-induced carotid artery occlusion in mice. *J Thromb Haemost.* **2005**, 3, 695-702.

(6) (a) Quan, M. L.; Wong, P. C.; Wang, C.; Woerner, F.; Smallheer, J. M.; Barbera, F. A.; Bozarth, J. M.; Brown, R. L.; Harpel, M. R.; Luetzgen, J. M.; Morin, P. E.; Peterson, T.; Ramamurthy, V.; Rendina, A. R.; Rossi, K. A.; Watson, C. A.; Wei, A.; Zhang, G.; Seiffert, D.; Wexler, R. R. Tetrahydroquinoline derivatives as potent and selective factor XIa inhibitors. *J. Med. Chem.* **2014**, 57, 955-969. (b) Smallheer, J. M.; Wang, S.; Rossi, K. A.; Rendina, A. R.; Morin, P. E.; Wei, A.; Zhang, G.; Wong, P. C.; Seiffert, D.; Wexler, R. R.; Quan, M. L. Biaryl methyl indoline and indole

analogs as potent and selective inhibitors of factor XIa. Presented at the 245th National Meeting of the American Chemical Society, New Orleans, LA, April 2013; MEDI-415. (c) Hangeland, J. J.; Friends, T. J.; Rossi, K. A.; Smallheer, J. M.; Wang, C.; Sun, Z.; Corte, J. R.; Fang, T.; Wong, P. C.; Rendina, A. R.; Barbera, F. A.; Bozarth, J. M.; Luetttgen, J. M.; Watson, C. A.; Zhang, G.; Wei, A.; Ramamurthy, V.; Morin, P. E.; Bisacchi, G. S.; Subramaniam, S.; Arunachalam, P.; Mathur, A.; Seiffert, D. A. Wexler, R. R.; Quan, M. L. Phenylimidazoles as potent and selective inhibitors of coagulation factor XIa with in vivo antithrombotic activity. *J Med Chem.* **2014**, 57, 9915-9932. (d) Pinto, D. J. P.; Smallheer, J. M.; Corte, J. R.; Austin, E. J. D.; Wang, C.; Fang, T., Smith, L. M.; Rossi, K. A.; Rendina, A. R.; Bozarth, J. M.; Zhang, G.; Wei, A.; Ramamurthy, V.; Sheriff, S.; Myers, J. E.; Morin, P. E.; Luetttgen, J. M.; Seiffert, D. A.; Quan, M. L.; Wexler, R. R. Structure-based design of inhibitors of coagulation factor XIa with novel P1 moieties. *Bioorg. Med. Chem. Lett.* **2015**, 25, 1635-1642. (e) Hu, Z.; Wong, P. C.; Gilligan, P. J.; Han, W.; Pabbisetty, K. B.; Bozarth, J. M.; Crain, E. J.; Harper, T.; Luetttgen, J. M.; Myers, J. E.; Ramamurthy, V.; Rossi, K. A.; Sheriff, S.; Watson, C. A.; Wei, A.; Zheng, J. J.; Seiffert, D. A.; Wexler, R. R.; Quan, M. L. Discovery of a potent parenterally administered factor XIa inhibitor with hydroxyquinolin-2(1H)-one as the P2' moiety. *ACS Med. Chem. Lett.* **2015**, 6, 590-595. (f) Corte, J. R.; Fang, T.; Hangeland, J. J.; Friends, T. J.; Rendina, A. R.; Luetttgen, J. M.; Bozarth, J. M.; Barbera, F. A.; Rossi, K. A.; Wei, A.; Ramamurthy, V.; Morin, P. E.; Seiffert, D. A.; Wexler, R. R.; Quan, M. L. Pyridine and pyridinone-based factor XIa inhibitors. *Bioorg. Med. Chem. Lett.* **2015**, 25, 925-930. (g) Corte, J. R.; Fang, T.; Pinto, D. J. P.; Orwat, M. J.; Rendina, A. R.; Luetttgen, J. M.; Rossi, K. A.; Wei, A.; Ramamurthy, V.; Myers, J. E.; Sheriff, S.; Narayanan, R.; Harper, T. W.; Zheng, J. J.; Li, Y.; Seiffert, D. A.; Wexler, R. R.; Quan, M. L. Orally bioavailable pyridine and pyrimidine-based factor XIa inhibitors: discovery of the methyl *N*-phenyl carbamate P2 prime

group. *Bioorg. Med. Chem. Lett.* **2016**, *24*, 2257-2272. (h) Smith, L. M.; Orwat, M. J.; Hu, Z.; Han, W.; Wang, C.; Rossi, K. A.; Gilligan, P. J.; Pabbisetty, K. B.; Osuna, H.; Corte, J. R.; Rendina, A. R.; Luettgen, J. M.; Wong, P. C.; Narayanan, R.; Harper, T. W.; Bozarth, J. M.; Crain, E. J.; Wei, A.; Ramamurthy, V.; Morin, P. E.; Xin, B.; Zheng, J.; Seiffert, D. A.; Quan, M. L.; Lam, P. Y. S.; Wexler, R. R.; Pinto, D. J. P. Novel phenylalanine derived diamides as factor XIa inhibitors. *Bioorg. Med. Chem. Lett.* **2016**, *26*, 472-478. (i) Deng, H.; Bannister, T. D.; Jin, L.; Babine, R. E.; Quinn, J.; Nagafuji, P.; Celatka, C. A.; Lin, J.; Lazarova, T. I.; Rynkiewicz, M. J.; Bibbins, F.; Pandey, P.; Gorga, J.; Meyers, H. V.; Abdel-Meguid, S. S.; Strickler, J. E. Synthesis, SAR exploration, and x-ray crystal structures of factor XIa inhibitors containing an α -ketothiazole arginine. *Bioorg. Med. Chem. Lett.* **2006**, *16*, 3049-3054. (j) Lin, J.; Deng, H.; Jin, L.; Pandey, P.; Quinn, J.; Cantin, S.; Rynkiewicz, M. J.; Gorga, J. C.; Bibbins, F.; Celatka, C. A.; Nagafuji, P.; Bannister, T. D.; Meyers, H. V.; Babine, R. E.; Hayward, N. J.; Weaver, D.; Benjamin, H.; Stassen, F.; Abdel-Meguid, S. S.; Strickler, J. E. Design, synthesis, and biological evaluation of peptidomimetic inhibitors of factor XIa as novel anticoagulants. *J. Med. Chem.* **2006**, *49*, 7781-7791. (k) Boronic acid peptidomimetics and the natural product clavatadine A are also examples of active site irreversible FXIa inhibitors but they have not been studied in preclinical thrombosis models, please see Lazarova, T. I.; Jin, L.; Rynkiewicz, M.; Gorga, J.C.; Bibbins, F.; Meyers, H. V.; Babine, R.; Strickler, J. Synthesis and in vitro biological evaluation of aryl boronic acids as potential inhibitors of factor XIa. *Bioorg. Med. Chem. Lett.* **2006**, *16*, 5022-5027. (l) Buchanan, M. S.; Carroll, A. R.; Wessling, D.; Jobling, M.; Avery, V. M.; Davis, R. A.; Feng, Y.; Xue, Y.; Oster, L.; Fex, T.; Deinum, J.; Hooper, J. N. A.; Quinn, R. J. Clavatadine A, a natural product with selective recognition and irreversible inhibition of factor XIa. *J. Med. Chem.* **2008**, *51*, 3583-3587. (m) Al-Horani, R. A.; Desai, U. R. Designing allosteric inhibitors of factor XIa.

Lessons from the interactions of sulfated pentagalloylglucopyranosides. *J. Med. Chem.* **2014**, *57*, 4805-4818. (n) An active site reversible FXIa inhibitor based on a diamide chemotype was also recently disclosed, please see: Fjellström, O.; Akkaya, S.; Beisel, H-G.; Eriksson, P-O.; Erixon, K.; Gustafsson, D.; *et al.* Creating Novel Activated Factor XI Inhibitors through Fragment Based Lead Generation and Structure Aided Drug Design. *PLoS ONE* **2015**, *10*, e0113705.

(7) (a) Yamashita, A.; Nishihira, K.; Kitazawa, T.; Yoshihashi, K.; Soeda, T.; Esaki, K.; Imamura, T.; Hattori, K.; Asada, Y. Factor XI contributes to thrombus propagation on injured neotima of the rabbit iliac artery. *J. Thromb. Haemost.* **2006**, *4*, 1496-1501. (b) Tucker, E. I.; Marzec, U. M.; White, T. C.; Hurst, S.; Rugonyi, S.; McCarty, O. J. T.; Gailani, D.; Gruber, A.; Hanson, S. R. Prevention of vascular graft occlusion and thrombus-associated thrombin generation by inhibition of factor XI. *Blood* **2009**, *113*, 936-944. (c) Gruber, A.; Hanson, S. R. Factor XI-dependence of surface-and tissue-initiated thrombus propagation in primates. *Blood* **2003**, *102*, 953-955.

(8) (a) Crosby, J. R.; Marzec, U.; Revenko, A. S.; Zhao, C.; Gao, D.; Matafonov, A.; Gailani, D.; MacLeod, A. R.; Tucker, E. I.; Gruber, A.; Hanson, S.; Monia, B. P. Antithrombotic effect of antisense factor XI oligonucleotide treatment in primates. *Arterioscler. Thromb. Vasc. Biol.* **2013**, *33*, 1670-1678. (b) Zhang, H.; Lowenberg, E. C.; Crosby, J. R.; MacLeod, A. R.; Zhao, C.; Gao, D.; Black, C.; Revenko, A. S.; Meijers, J. C. M.; Strokes, E. S.; Levi, M.; Monia, B. P. Inhibition of the intrinsic coagulation pathway factor XI by antisense oligonucleotides: a novel antithrombotic strategy with lowered bleeding risk. *Blood* **2010**, *116*, 4684-4692. (c) Buller, H. R.; Bethune, C.; Bhanot, S.; Gailani, D.; Monia, B. P.; Raskob, G. E.; Segers, A.; Verhamme, P.; Weitz, J. I. Factor XI antisense oligonucleotide for prevention of venous thrombosis. *N. Engl. J. Med.* **2015**, *372*, 232-240. An alternative name for IONIS-FXIRx is BAY-2306001.

- (9) Wong, P. C.; Quan, M. L.; Watson, C. A.; Crain, E. J.; Harpel, M. R.; Rendina, A. R.; Luetttgen, J. M.; Wexler, R. R.; Schumacher, W. A.; Seiffert, D. A. In vitro, antithrombotic and bleeding time studies of BMS-654457, a small-molecule, reversible and direct inhibitor of factor XIa. *J. Thromb. Thrombolysis* **2015**, *40*, 416-423
- (10) (a) Váradi, A.; Palmer, T. C.; Dardashti, R. N.; Majumdar, S. Isocyanide-Based Multicomponent Reactions for the Synthesis of Heterocycles. *Molecules* **2016**, *21*, 1-22. (b) Müller, T. J. J. In Multicomponent Reactions 1. General Discussion and Reactions Involving a Carbonyl Compound as Electrophilic Component; Müller, T. J. J., Ed.; Science of Synthesis Series; Georg Thieme Verlag KG: Stuttgart, **2014**, 5–27(11) (a) Wong, P. C.; Quan, M. L.; Crain, E. J.; Watson, C. A.; Wexler, R. R.; Knabb, R.M. Nonpeptide factor Xa inhibitors: I. Studies with SF303 and SK549, a new class of potent antithrombotics. *J. Pharmacol. Exp. Ther.* **2000**, *292*, 351–357. (b) Wong, P. C.; Crain, E. J.; Watson, C. A.; Hua, J.; Schumacher, W. A.; Rehfuss, R. Clopidogrel versus prasugrel in rabbits: Effects on thrombosis, hemostasis, platelet function and response variability. *Thromb Haemost.* **2009**, *101*, 108-115
- (12) (a) Luetttgen, J. M.; Wong, P. C.; Perera, V.; Wang, Z.; Russo, C.; Chen, W.; Dorizio, S. M.; Frost, C. E.; Dierks, E.; Pinto, D. J. P.; Ewing, W. R.; Wexler, R. R.; DeSouza, M. M.; LaCreta, F. P.; Gordon, D. A.; Seiffert, D. A.; Frost R. J. Preclinical and Early Clinical Characterization of a Parenterally Administered Direct Factor XIa Inhibitor. *Stroke*, **2017**, *48*, TMP117. (b) Perera V.; Frost C. E.; Yones, C. L.; Wang, Z.; Dorizio, S.; Russo, C.; Chen, W.; Ueno, T.; Akimoto, M. Cirincione, B.; Xu, X.; Seiffert, D. A.; Desouza, M. M.; Mugnier, P.; LaCreta, F.; Frost, R. J. Pharmacokinetics, Pharmacodynamics, Safety and Tolerability of a Novel Factor XIa Inhibitor Administered as IV Infusion in Non-Japanese and Japanese Healthy Subjects. (2017), American Society for Clinical Pharmacology and Therapeutics. *Clin. Pharmacol. Ther.*, **2017**, *101*, S5–S99

- (13) Blessing, R. H. An Empirical Correction for Absorption Anisotropy. *Acta Crystallogr. Sect A* **1995**, *51*, 33-38.
- (14) Sheldrick, G. M. A short history of SHELX. *Acta Crystallogr. Sect. A* **2008**, *64*, 112-122.
- (15) Otwinowski, Z.; Minor, W. Macromolecular Crystallography. Part A, in *Methods in Enzymology*, Carter, C. W., Jr.; Sweet, R. M., Eds.,; Academic Press: New York, NY, **1997**, Vol. 276, pp 307–326.
- (16) Blanc, E.; Roversi, P.; Vonrhein, C.; Flensburg, C.; Lea, S. M.; Bricogne, G. Refinement of severely incomplete structures with maximum likelihood in BUSTER/TNT. *Acta Crystallogr., Sect. D: Biol. Crystallogr.* **2004**, *60*, 2210–2221.
- (17) Emsley, P.; Lokhamp, B.; Scott, W. G.; Cowtan, K. Features and development of Coot. *Acta Crystallogr., Sect. D: Biol. Crystallogr.* **2010**, *66*, 486–501.
- (18) Kabsch, W. *Acta Crystallogr. Sect. D: Biol. Crystallogr.* 2010, *66*, 125-132; Kabsch, W. *Acta Crystallogr. Sect. D: Biol. Crystallogr.* 2010, *66*, 133-144.
- (19) Evans, P.R., Murshudov, G.N. *Acta Crystallogr. Sect. D: Biol. Crystallogr* 2013, *69*, 1204-1214.
- (19) Laskowski, R. A.; MacArthur, M. W.; Moss, D. S. & Thornton, J. M. *PROCHECK*: a program to check the stereochemical quality of protein structures. *J. Appl. Crystallogr.* **1993**, *26*, 283-291.

TABLE OF CONTENTS GRAPHIC

